FACULDADE DE ENGENHARIA DA UNIVERSIDADE DO PORTO

Organic structures under pressure – Experimental validation of a testing device with application to arterial and vascular mechanics

Renata Daniela Ferreira Couto

MASTER'S THESIS

MESTRADO INTEGRADO EM BIOENGENHARIA

Supervisor: Pedro Alexandre Lopes de Sousa Martins

Cossupervisor: Renato Manuel Natal Jorge

June 12, 2018

Resumo

As doenças cardiovasculares são a principal causa de morte no mundo e é previsível que assim continue, devido à má alimentação da população e ao constante aumento mundial da taxa de obesidade. Um dos tratamentos para este grupo de doenças é a Intervenção Percutânea Coronária, que normalmente precede a colocação de um stent arterial.

Com o desenvolvimento da ciência, a tecnologia deste dispositivo médico tem sofrido um grande desenvolvimento e o primeiro tipo de stents arteriais foi substituído por outro, mais recente, e com melhores resultados. No entanto, foi provado que os benefícios dos stents da nova geração, comparados com os da geração mais antiga, não trazem uma melhoria significativa à vida dos pacientes. É desta lacuna da investigação médica que surge a oportunidade de investigar como é que os stents de primeira geração podem ser redesenhados e melhorados, por forma a tornarem-se de novo o tipo de stents arteriais mais recomendado.

De modo a ser possível avançar com esta investigação, houve a necessidade de desenvolver o dispositivo de teste apresentado nesta dissertação. Tendo este sido testado na inflação de balões longos (com forma semelhante à das artérias) e num pedaço de aorta suína, tendo estas estruturas sido pressurizadas com sucesso, conclui-se que este dispositivo pode ser usado para estudar diferentes sistemas e tecidos. No entanto, o principal foco será o estudo das propriedades mecânicas das artérias e, no futuro, no estudo do comportamento do conjunto composto pela artéria e pelo stent.

Abstract

Cardiovascular diseases are the leading cause of death worldwide and it is predictable that this will continue over the years due to the poor diet of people and the rising rate of obesity. One of the treatments for these group of pathologies is the Percutaneous Coronary Intervention, which normally precedes the placement of an arterial stent.

The technology of these medical devices has undergone major development and the first arterial stents produced have been replaced by others with better results. However, it has been proven that the benefits of newer stents, compared with older ones, do not bring a significant improvement to patients' lives. It is from this research gap that arises the opportunity to investigate how first-generation stents can be redesigned to become again the gold standard for this type of medical device.

To advance this study, it was necessary to develop the Injection Pump device, presented in this dissertation. The apparatus was used to inflate long balloons and a piece of porcine aortic, having these structures been pressurized with success. So, it can be concluded that this device can be used to study different systems and tissues. However, the main bet will be in the study of the mechanical properties of the arteries and, in the future, the behaviour of the set composed by the artery and the stent.

Acknowledgments

The following words are not enough to thank all those who have made it possible to carry out this work. I have to thank my supervisor, doctor Pedro Martins, for the opportunity he gave by letting me integrate a project related with biomechanics/biomaterials and for all the support and advice throughout these 2 years.

To Fundação para a Ciência e Tecnologia for financing the construction of the device from scratch, through the project Urosphinx, and to Francisco Pereira, who was part of the research team.

A special thanks to Sérgio Pinto and António Diogo André, who always assisted me in solving the electronic and mechanical problems related to the Injection Pump device.

To my family and friends: thank you for always being on my side and for the support and motivation you have always given me.

To finish, my parents and my boyfriend, who have always helped me to overcome the most difficult moments, always having the right words of comfort to tell me in those moments.

Renata Couto

Contents

List of Figures

List of Tables

Abbreviations and Symbols

BMS	Bare Metal Stents
BVS	Bioresorbable Vascular Scaffold
cm^3	Cubic Centimeters
DES	Drug Eluting Stents
DTS	Dual Therapy Stent
EPCs	Endothelial Progenitor Cells
kPa	KiloPascal
mm^3	Cubic Millimeters
mm Hg	Millimeters of Mercury
Pa	Pascal
PCI	Percutaneous Coronary Intervention

Chapter 1

Introduction

1.1 Context

Cardiovascular diseases is a group of diseases that involve the heart and the blood vessels and, in 2015, 17.7 million people died from this disease, representing 31% of all global deaths making it the leading cause of death in the world [10].

The phenomenon responsible for these diseases is atherosclerosis which is characterized by the build-up of plaques inside of arteries. This plaques are made up of fat, cholesterol and other substances found in the blood. Over time, the plaques become larger and narrows the arteries which reduces the flow of blood to the organs and other parts of the body [11].

One available treatment for atherosclerosis is Percutaneous Coronary Intervention (PCI), which is a procedure that opens blocked or narrowed arteries and this is made to re-establish the normal blood and oxygen flow. To prevent the restenosis of the artery, that is, to keep the artery open after the surgery and prevent its collapse, a medical device called stent is placed in the site of obstruction [12].

1.2 Motivation

The investigation of the mechanobiological behaviour of arteries in health and disease is a central aim in cardiovascular solid mechanics. Understanding this behaviour is critical for the treatment of arterial diseases, for tissue engineering and for the design of vascular implants such as grafts and stents.

Although there are currently several types of arterial stents, the first to be produced are not the gold standard of these medical devices anymore, despite the benefits of their use are clearly greater when compared to more recent designs.

In this way, it is essential to investigate how to change the design and properties of these devices in order to make them again the most used type of stents. For this, it is necessary to better explore the mechanical properties of the arteries to improve the understanding of stent designs.

This was the reason that led to the development of the testing device presented in this dissertation. It will be used to perform inflation tests in the arteries and, later, in the artery + stent assembly, and evaluate their behaviour. The results will allow to understand how to improve the stents under study.

1.3 Objectives

The main goal of this dissertation is to validate experimentally a testing device for organic tissues under pressure. The inspiration for its creation was the study of the vascular system, in particular the arteries, but it can be easily used in other soft tissues and systems such as the urinary system, to study the urethra, for instance.

The main components of this system have already been developed. Thus, the proposed objectives for the validation of the system are: (i) assemble an automated testing system for pressured biological systems; (ii) validate the testing system; (iii) create an experimental protocol, for biological materials, adapted to the system and (iv) perform the mechanical characterization of biological vessels (arteries or veins) as test/application proof of the system.

1.4 Document Structure

The remaining document is structured as: in Chapter 2, is presented a brief summary of the structural constitution of the arteries, the literature review of the experimental tests and mechanical behaviour of vascular and arterial tissues and the main conclusions; in Chapter 3 the Injection Pump device is explained in detail and the upgrade made in the Matlab interface that controls the apparatus is described, as well as the innovative method that was used to attach the specimen under study to the device; in Chapter 4 the methodology followed to perform the inflation tests to the long balloons and to the organic structures is reported; in Chapter 5 are presented the results of the tests and the discussion of the results; lastly, in Chapter 6 can be found the main conclusions from this dissertation and the future work that can be done in order to improve this work.

Chapter 2

Literature Review

Throughout this chapter, is not only presented a short summary of the structure of the arteries but also a literature review of the experimental tests and mechanical behaviour of vascular and arterial tissues. The state of the art presented is divided according to the type of test used, that is, if it was performed an extension/compression test, an inflation test or an extension-inflation test. Once the aim of this dissertation is the experimental validation of a testing device for conducting inflation tests, a brief mention is done to the apparatus used by the different authors in their works.

The existing types of stents and the surrounding technology are also described. Lastly, at the end of the chapter there are the final conclusions.

2.1 Structural constitution of arteries

Blood vessels are the channels where the blood circulates and is distributed on the tissues. There are two circulatory systems: one that transports arterial blood, from the right ventricle to the lungs and back to the left atrium and the other system carries the blood from the left ventricle to the tissues and then back to the right atrium. Depending on the function and structure, blood vessels are classified in arteries, capillaries or veins.

The main vessel of interest in this dissertation is the artery. Arteries carry blood away from the heart. The wall of an artery is composed of three layers, all of which have different mechanical properties and play a different role. These layers are the tunica intima, the tunica media and the tunica adventitia and are represented in Figure 2.1.

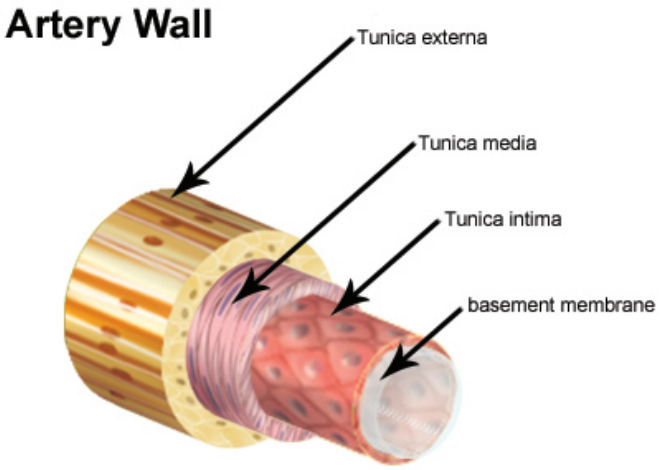

Figure 2.1: Artery wall composition [1].

The innermost layer is the tunica intima which is a prominent layer composed by connective tissue, collagen and elastic fibres. The second one, the tunica media, is the middle layer and is essentially smooth muscle, collagen and elastic fibres, being the thickest layer. It provides support for the vessel and its diameter is variable, in order to regulate the blood flow and pressure. The outermost layer is the tunica adventitia, which contacts directly with the blood, and consists in an elastic membrane with collagen fibres and smooth endothelial cells [13, 1].

2.2 Mechanical behaviour of vascular and arterial tissue

The knowledge of the mechanics and pathophysiology of the cardiovascular system goes through the perfect understanding of the stresses and strain developed in arterial walls, which cannot be analyzed without the mechanical properties of the arterial wall [14].

Extension and inflation tests of arteries are essential to measure these mechanical properties. Despite the cardiovascular system being one of the most important in biomechanics, data on extension and inflation behaviour of arteries are rare [7].

2.2.1 Extension/compression tests

A tensile test is performed when the behaviour of materials, tissues in this case, under axial tensile loading needs to be studied. In these tests, the specimen is fixed in the testing device and a force is applied, separating the testing machine crossheads. The speed of the movement can be chosen according to the rate of strain applied to the specimen. This type of test allows the calculation of mechanical properties of materials, such as the yield strength, the tensile strength and the modulus of elasticity [15].

[16] applied a uniaxial compressive force on rabbit thoracic arteries, in the radial direction, in order to study the elastic behaviour of the arteries when subjected to compressive forces. Another

aim of the work was to measure the amount of fluid extruded from the vessel in those conditions. The results of stress-strain curves showed that the greater the compressive strain, the greater the stiffness of the arterial wall. It was demonstrated that fluid extrusion was 0.5-1.26 percent of the underformed tissue volume per 10kPa compressive stress. As major conclusion, they found that the arterial wall is nearly incompressible.

[13] studied the properties of each layer of the wall of human coronary arteries. They performed uniaxial tensile tests and measured the stretches and ultimate tensile stresses. The stretches-stresses curves confirmed mechanical heterogeneity. One of the discoveries made by the authors was that the media is the softest layer of the arterial wall in the longitudinal direction and the intima is the stiffest.

[17] performed uniaxial and equibiaxial tension tests in porcine coronary arteries in order to study their nonlinear anisotropic elastic behaviour. The anisotropy of the tissue was demonstrated once the testing device applied an equal force to the four sides of the arterial segment, which created a biaxial stretch. The nonelastic behaviour was demonstrated in both biaxial and uniaxial tests. The results showed that the tissue is stiffer in circumferential direction.

The mechanical properties of healthy and atherosclerotic human coronary arteries were investigated by [18]. The maximum stress, maximum strain, physiological and maximum elastic modulus of the human arteries were measured, the force-displacement diagram was obtained and the difference between the stiffness of both arterial walls was evaluated. To make this assessment, force was applied on the arterial tissue until breakage occurs and the elastic modulus coefficient of each specimen was calculated. The authors found that, compared to the healthy ones, the atherosclerotic arteries bear 44.55% more stress and 34.61% less strain and the maximum and physiological elastic moduli of healthy arteries are, respectively, 2.53 and 2.91 times higher than that of atherosclerotic arteries, meaning that healthy arteries are stiffer.

2.2.2 Inflation tests

Inflation tests are performed on the materials when the desire is to evaluate their behaviour, at different pressures. Uniaxial and biaxial tests are often performed on flat specimens to determine the mechanical properties of arterial walls. However, inflation tests are more informative and realistic because reflects the motion of the aortic wall during the cardiac cycle [14, 9].

[2] studied the anisotropy and behaviour of arterial walls using femoral, abdominal and common carotid arteries of mongrel dogs. The specimens were stretched, keeping the internal pressure at different levels and a movie camera was used to measure the external diameter of the specimen and its displacement in axial direction. The apparatus used is presented in Figure 2.2.

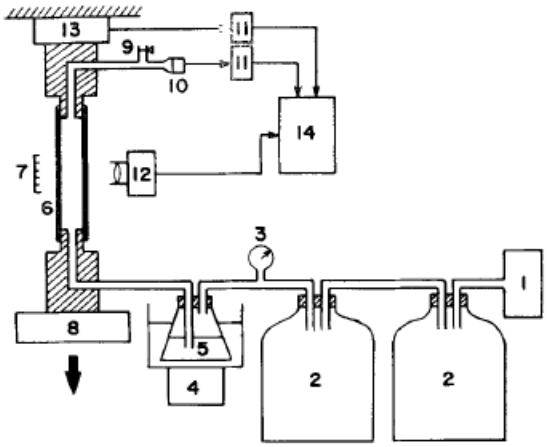

Figure 2.2: Testing device used by [2].

The authors concluded that the internal pressure applied to the arteries is related to their mechanical properties, being these properties dependent on the pressure. The most dependent is the abdominal aorta and the anisotropic mechanical behaviour of the arteries was confirmed.

Pressure-diameter tests were performed, by [3], in excised thoracic aortas, common carotid and femoral arteries of rabbits to evaluate the effects of cholesterol feeding and elastase administration on the elastic properties and arterial stiffness. The vessels segments were inflated, the external diameter was measured by a television system, consisting of a vidicon camera and a width analyzer, and the intraluminal pressure was measured with a pressure transducer (Figure 2.3.).

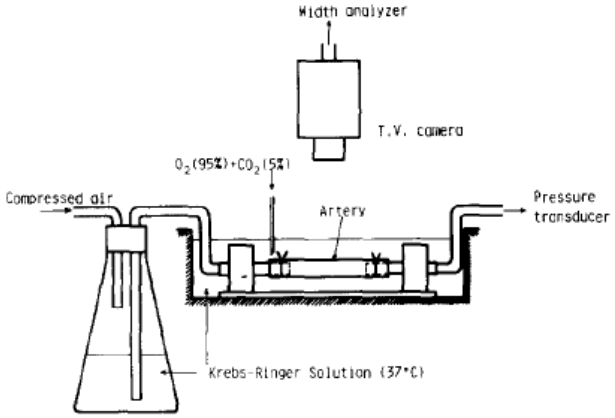

Figure 2.3: Schematic representation of the testing apparatus used by [3].

The results showed that both stiffness and elastic modulus of major arteries were higher in the cholesterol-fed rabbits than in the control group. The administration of elastase decreases the stiffness, result of the decrease of the elastic modulus of the arteries.

The variations in the external radius of three different arterial walls, due to distending pressure, were studied by [4] to understand their static behaviour, examining the distensibility of these vessels. The specimen diameter was measured with a photocell combined with light emitting diode (Figure 2.4.).

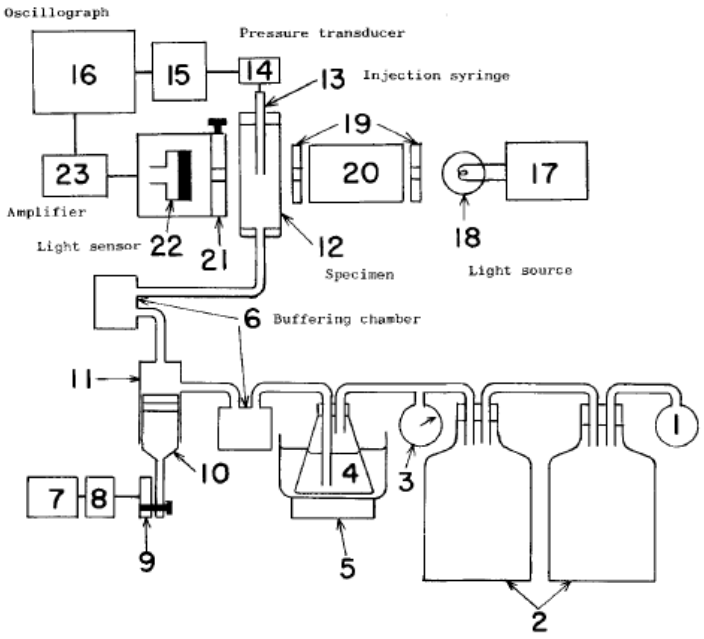

Figure 2.4: Testing device used by [4].

It was possible to conclude that to low-pressure ranges, below 50 mmHg, the wall radius increases the pressure, to pressures between 50 and 150 mmHg, the wall became stiffer and to pressures above 150 mmHg, the distensibility was lost.

[19] investigated the effects of aging and smooth muscle activation on the elastic stiffness of the aortic wall of 9 anesthetized sheep, measuring the aortic pressure and the external aortic diameters. This measurement was made with an ultrasound technique which measures the transit time of acoustic impulses with a velocity of 1.5x106 mm/s between pairs of the implanted piezoelectric crystals. This system provides a continuous and instantaneous measure of the external vessel diameter. The results showed that the modulus of elasticity of the aorta of the young adult sheep is higher than that of the newborn lamb, due to the first ones being subject to higher levels of stress. Nevertheless, when the level of stresses is the same, the aorta of the adult sheep has lower elastic modulus.

[20] had as motivation of their study the elasticity of canine and human coronary arteries. The authors started their work with a study on the elasticity changes of the femoral artery after excision and cold storage. This step was necessary because they had to use postmortem material to study human arteries. The dynamic and static incremental elastic modulus were calculated from pressure diameter traces. In this work, a caliper was sewn onto the adventitia to measure the diameter of

the vessel. The authors concluded not only that both dynamic and static elastic modulus are higher after excision and cold storage, for human arteries, but also that the dynamic elastic modulus of the femoral artery is the same as the canine left circumflex coronary artery.

[5] created an apparatus (Figure 2.5.) to measure the transmural pressure, diameter and longitudinal force in real-time, of sheep common carotid artery segments, *in vitro*.

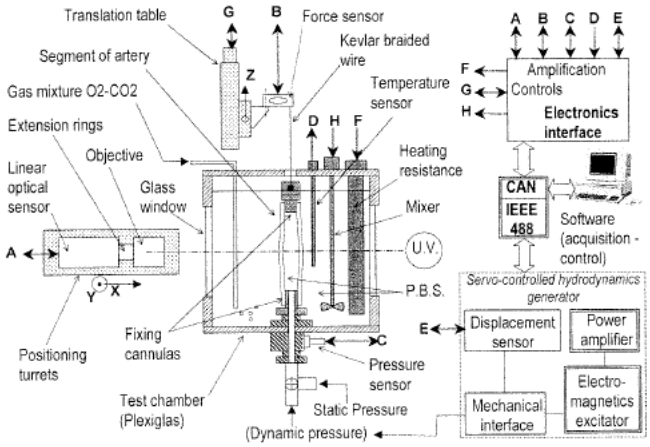

Figure 2.5: Device created by [5].

The aim of their work was to investigate the 3D mechanical properties of blood vessels with the new experimental device they have designed. After applying static tests to the specimens, they calculated the mechanical properties and concluded that their results were in agreement with the published results. The stress-strain curves obtained are in the physiological range of pressure and it was confirmed that the sheep common carotid artery has an anisotropic behaviour.

The elastic and rupture properties of porcine aortic tissue were investigated by [21]. They developed a new inflation test device, measured the failure strength and determined the nonlinear and anisotropic elastic properties of porcine thoracic aorta. It was possible to conclude that the isotropic contribution to constitutive model was insignificant and that the dominant directions of anisotropy were 45^{o} to axial and circumferential directions.

[22] measured the burst pressure using an experimental setup that pressurizes the vascular construct and registers the applied pressure and the external diameter until failure. The pressure inside of the vascular construct was varied in the range of 70 to 130 mmHg, in order to simulate the physiological conditions. The assembly used is similar to the ones described above.

2.2.3 Extension-inflation tests

Sometimes extension and inflation tests are performed at the same time, in order to evaluate different mechanical properties of tissues.

The compressibility of the arterial wall was the object of study of [6]. They measured the changes in volume, associated with induced and large strain, in segments of excised dog aorta.

While the specimen was inflated and the longitudinal stretch was greater than those *in vivo*, the circumferential, radial and longitudinal stresses were recorded. The experimental setup used by the authors is represented in Figure 2.6.

The main result of the study is that the arteries may be considered incompressible since the greatest volume strain registered was 0.00165.

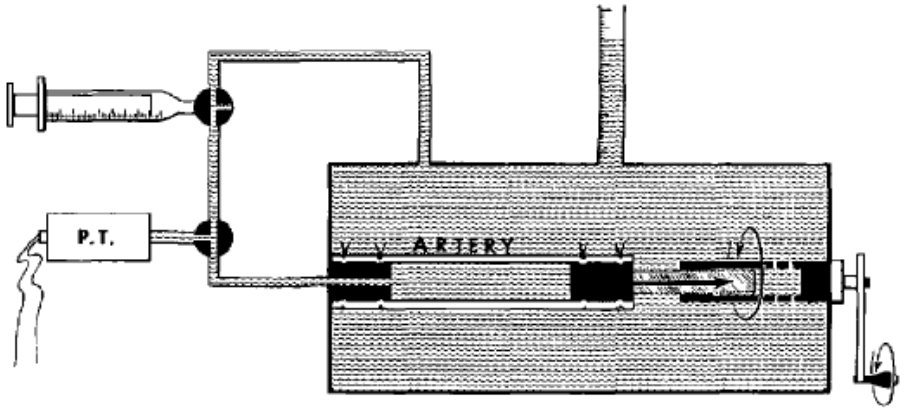

Figure 2.6: Experimental setup used by [6].

[7] investigated essential characteristics of passive biaxial mechanical responses of aged human iliac arteries by means of quasistatic tube tests of fresh specimens and performed 2D recordings of vessel deformations, within a range of axial loads and inflation pressures. To conduct this study, the authors used an experimental setup composed by a video-based deformation measurement system, a test cage, a system which was used to generate and measure pressure and a data acquisition system based on a PC. The experimental setup is represented in Figure 2.7.

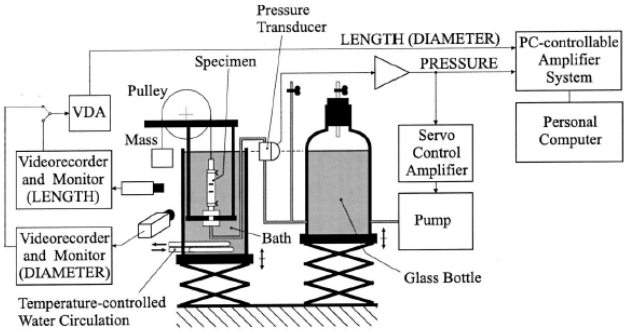

Figure 2.7: Experimental setup adopted by [7].

With this study, it was possible to conclude that the three layers of the arterial wall exhibit greater thickness and mechanical strength than animal specimens. Another finding is that it is necessary to undergo *in situ* inflations, with mean arterial pressure, to determine more accurately the physiological operation range of arteries with small axial stretch.

[8] had as object of study the biaxial anisotropy of dog carotid arteries. The segments were subjected to a wide range of longitudinal lengths and transmural pressures. For different lengths, the pressure inside the specimens was increased in 25 mmHg steps up to 200 mmHg, or until the traction force was zero. A linear displacement transducer was used to measure the diameter of the vessel (Figure 2.8.).

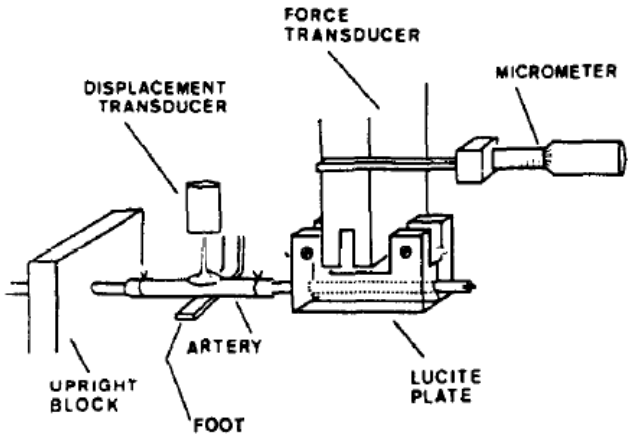

Figure 2.8: Apparatus and experimental method of [8].

The possible conclusions were that the longitudinal extension increases the longitudinal elastic modulus but does not affect the circumferential modulus. The vessels are nearly isotropic at physiological pressures but at shorter lengths are anisotropic. When corrected, the pressure elastic modulus can be used to estimate the anisotropic modulus of carotid arteries.

[23] studied adventitia mechanics using a thin-walled model. The extension-inflation tests were performed in two different domains: the physiological and the higher pressure domain. The outer diameter was registered with a videoextensometer using a CCD camera and the pressure using a strain-gauge pressure transducer. The tests showed that adventitia has a nearly elastic behaviour, for both domains, and have the greatest tensile strength. 2D Fung-type stored-energy functions represents the anisotropic and nonlinear mechanical responses of the adventitia.

[9] developed an extension-inflation experimental setup to study the circumferential variations in mechanical properties of 4 regions of the porcine thoracic aorta. This apparatus was constituted by a stereo vision system and a stress-strain analysis method and it is presented in Figure 2.9.

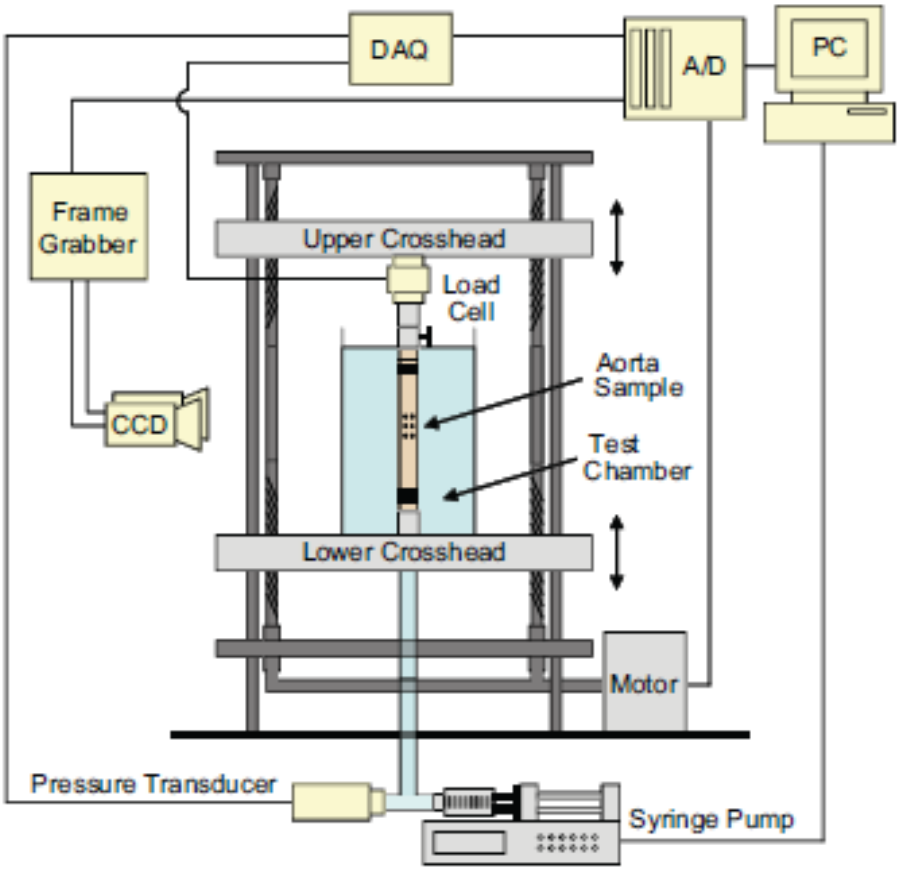

Figure 2.9: Schematic diagram of the experimental setup developed by [9].

With this study it was found that the posterior region of the porcine thoracic aorta is stiffer than the anterior, despite the posterior region is thinner. Limitations of this approach may be related to the rotation of the aorta when measuring the strain at the four circumferential regions of the aorta. The aorta must be fixed and it is the system that moves.

2.3 Stents

As was previously mentioned in the Chapter 1, the motivation of this dissertation is to understand how the first type of arterial stents may be modified, in order to improve its mechanical properties and thus the response of the human organism when the stent is implanted in an artery.

A stent is a tiny wire mesh tube [24] and this technology was introduced by Sigwart, in 1987 [25]. These medical devices are used to open an artery when it is narrowed by plaques of fat or other substances, which reduces the blood flow to the heart and causes chest pain. If there is a clot formation that blocks the artery permanently, the blood flow to the heart is suppressed,

which causes a heart attack. The stent is left permanently in the blood vessels to keep it open and prevent chest pain and heart attacks [24].

Currently, there are five types of arterial stents: Bare Metal Stents (BMS), Drug Eluting Stents (DES), Bio-engineered Stent, Bioresorbable Vascular Scaffold (BVS) and Dual Therapy Stent (DTS) [26].

2.3.1 Bare Metal Stents

BMS were the first type of these medical devices being produced, usually made of stainless steel (alloy 316 L), and are not coated. The second generation of BMS uses Cobalt-Chromium (Co-Cr) alloy [26].

The first stent approved by Food and Drug Administration, in June 1993, was called Gianturco-Roubin stent, in memory of its creators, Cesar Gianturco and Gary Roubin and it was made of 316 L stainless steel wire [27].

2.3.2 Drug Eluting Stents

DES are metallic stents coated with a polymer, which releases an antiproliferative medication. This drug is released with the aim of prevent the scar tissue in the artery lining, which ensures the artery remains open and the good blood flow, reducing the probability of restenosis. Among the most used medicines are: paclitaxel, everolimus, sirolimus and zotarolimus. One disadvantage of using this type of arterial stent is that the patients implanted with DES have the need to do Dual Antiplatelet Therapy (DAPT), for at least 12 months after the procedure, in order to prevent the risk of thrombosis [26].

2.3.3 Bio-engineered Stents

This type of arterial stents differs from DES because does not have a polymer or a drug but it is coated with a biocompatible matrix covered with antibodies, specific to the surface antigen present on circulating Endothelial Progenitor Cells (EPCs), generated in human bone marrow. The antibodies that are on its surface attract EPCs and these mature into endothelial cells. This process helps to speed up the endothelization, promoting the natural healing and reducing the risk of thrombosis due to the rapid stent coverage, by reducing the time the stent surface is exposed. The use of this type of stents only requires 4x per week of DAPT [26, 28].

2.3.4 Bioresorbable Vascular Scaffold

BVS provides medicine delivery and mechanical support functions similar to DES but have a complete resorption of the scaffold platform, which is absorbed by the body. The medicine is released from a polymer, which disappears over time and prevents the artery restenosis. BVS have not an active element to promote artery healing. It provides the recovery of normal vascular structure and function [26, 29].

2.3.5 Dual Therapy Stent

DTS is the most recent of this kind of medical devices and combines the properties of DES and Bio-engineered stent. The interior is coated with antibodies, using the technology of EPCs as in Bio-engineered stent, promoting the natural healing of the endothelium. The surface is coated with a bioresorbable polymer which releases a medicine, thereby preventing the artery to block again through the inhibition of neointimal formation. With these properties, DTS helps the healing process of the artery and decreases the likelihood of inflammation and blood clots [26, 30].

2.3.6 Improving BMS

After all the research presented above, it was possible to understand that the BMS are not the gold standard of the stent technology anymore. With the emergence of DES and all of the other types of these medical devices, these were set aside. However, and having as reference the study of [25], it is believed that it is still possible for BMS to be used as in the past. In their work, 9013 patients were randomly assigned to undergo PCI with implantation of BMS or DES and the long-term risks and benefits of the use of DES versus BMS were evaluated, in a large and randomized trial.

All patients followed the same procedure and had the same administration of medicine, before and after the implantation of the respective stent, according to the current guidelines, and were divided in two groups: a group composed by people who received BMS and another group with people who received DES.

The analysis of the outcomes showed no significant differences between the study groups in terms of rates of death from any cause, 6 years of follow-up. The rates of definitive stent thrombosis was low in both groups and the type of stent had no significant effect in the quality of life. However, it was detected a lower rate of revascularization and a lower rate of stent thrombosis in the group receiving DES.

Despite contemporary DES have a lower risk of stent thrombosis, when compared with BMS, did not translate into any difference in quality of life in the group receiving DES. In table 2.1 are presented the main differences between the outcomes of BMS and DES.

Table 2.1: Outcomes of BMS and DES

Outcome	BMS	DES
DAPT	1-2 months	12 months (at least)
Re-endothelization	About 100%	Almost non-existent
Late Stent Thrombosis	High rate	-
Very Late Stent Thrombosis	-	High rate
Restenosis	Between 15-20%	Around 10%
Sensibility to polymer	-	High
Vascular healing	After 4/6 months	Slow
Mortality rate	$\sim$40%	$\sim$40%
Major Adverse Cardiac Events	Large vessels	Narrow vessels

Given the results in table 2.1, no significantly differences were noticed between the outcomes of BMS and DES. Despite the difference in the restenosis rate, no other outcome presents a significant difference.

In relation to the duration of DAPT, the use of BMS is advised since its shorter, which is beneficial to patients with high risk of bleeding. It is also worth to highlight the re-endothelization rate that it is about 100% in BMS and almost null when DES are used. In regard to vascular healing, it is also more advantageous the utilization of BMS, since the recovery is complete 4/6 months after the procedure.

Comparing the results of using both medical devices, it can be said that many of the results of the BMS are superior to the DES. Changing the design so that the restenosis rate decreases, taking into account that all other results remain, it is possible to make BMS again the most used type of stents.

2.4 Conclusions

Throughout this chapter were summarized the panoply of experimental tests performed on human and animal arteries. A special emphasis has been placed on inflation tests and the different devices created over time, since the purpose of this dissertation is the experimental validation of a testing device with application to arterial and vascular mechanics. As has been described, such devices have wide application in the area of measurement of the mechanical properties of vascular segments or their substitutes.

The construction of the Injection Pump device thus arises with the need to investigate how the BMS can be redesigned and improved, so that they are again widely used. This led to the need of performing mechanical tests on arteries, to analyze their behaviour under pressure and, in the future, to analyze how the set composed by the artery and the stent behaves when subjected to physiological pressures.

The concept of the device is not completely new and the different unities of it are: (i) an inflation system, fully automated and programmable; (ii) pressure measurement, consisting of a direct measurement since the sensor is inside the vessel; (iii) deformation measurement, with 3D reconstruction of vessel deformation. Having these 3 components on a single solution is innovative and there is a huge potential to extend the same testing system to different biological systems, as the urinary system and study of the mechanical properties the urethra.

Chapter 3

The Injection Pump device

In this chapter is presented a section where the Injection Pump device is explained in detail. Two more sections make up this chapter: one where the improvement made in the Matlab interface, before all components of the system be assembled together, is described and another where it is explained how the object under study is attached to the device.

3.1 Inflation testing device

The Injection Pump, which is shown in Figure 3.1, is an inflation system testing device with application to organic structures under pressure. The apparatus is composed by three main components: an inflation system, a pressure measurement system and a deformation system. The device was developed to measure the transmural pressure of tubular structures, during the inflation test.

The Injection Pump is controlled from an interface in Matlab, where the user has to fill all the necessary parameters for the operation of the device. All three units were already developed, however, it was necessary to assemble them together.

A complete protocol of the use of the Injection Pump device was developed and may be consulted in chapter A. In this document is explained which are the softwares necessary to download, how to install the required libraries for the operation of the stepper motor and of the pressure sensor, what are the rules to use the Matlab interface and which are the resultant outputs of each test.

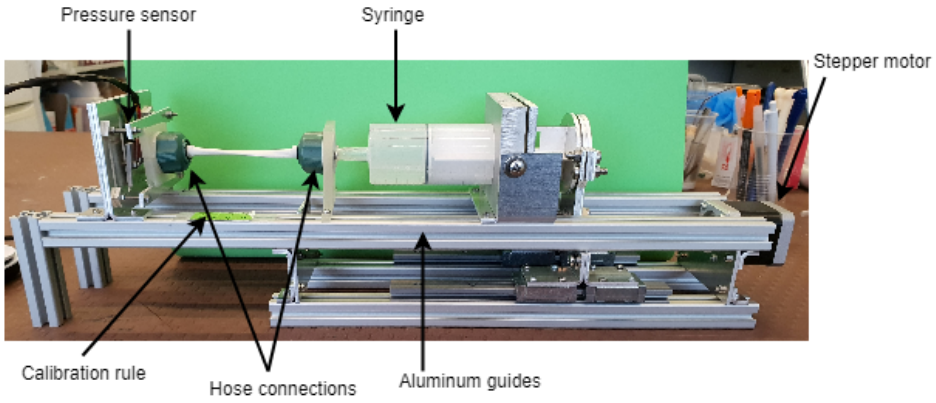

Figure 3.1: Injection Pump device.

3.1.1 Inflation system

The inflation system is composed by a stepper motor, a syringe and a worm screw. The operation of the stepper motor transmits motion to the screw which pushes the plunger of the syringe, that induces the pressurization or depressurization of the vascular object under study.

The stepper motor is controlled via Arduino (the code was already developed), that receives from Matlab the instructions that the user has provided by filling the interface. The specimen is connected, at one end, to the syringe by a hose connection.

3.1.2 Pressure measurement system

The pressure measurement system measures the transmural pressure using a pressure sensor with a range of 0-14 bar (MS5803-14BA). The transmural pressure was defined, by [9], as the difference in pressure between the outside and the inside of the specimen.

The sensor is connected to the specimen by a hose connection. The number of pressure measurements is set by the user (in the interface) and these are sent to Arduino that transmits the measurements made to Matlab, where the values are saved in a text file.

It was necessary to incorporate the pressure reading code into the stepper motor operating code and ensure that the measurements were performed the number of times the user asked.

3.1.3 Deformation system

Images are captured during the experience (at the same time that the transmural pressure is measured), using a normal camera (CANON PowerShot SX30 IS) and those images are used to perform the 3D reconstruction of the tubular structure and to calculate the volume of fluid inside it, with Fusion 360 software (from Autodesk).

The protocol of this unity was not yet developed so, the work was to perform a complete

methodology to reconstruct the tubular structure in each photo (that has different levels of deformation along the photos). The developed protocol can be consulted in chapter A, section A.2.3.3.

3.1.4 Outputs of each test

At the end of each test, one of the outputs is the set of images taken during the task - Figure 3.2 a). The number of images in the set is the number of transmural pressure readings (the user have defined) plus one, since the transmural pressure at the initial moment is measured too. The other output is a text file, generated by Matlab, which contains the instructions of that task (with the values attributed by the user to each parameter) and the transmural pressure values measured during the experience (Figure 3.2 b).

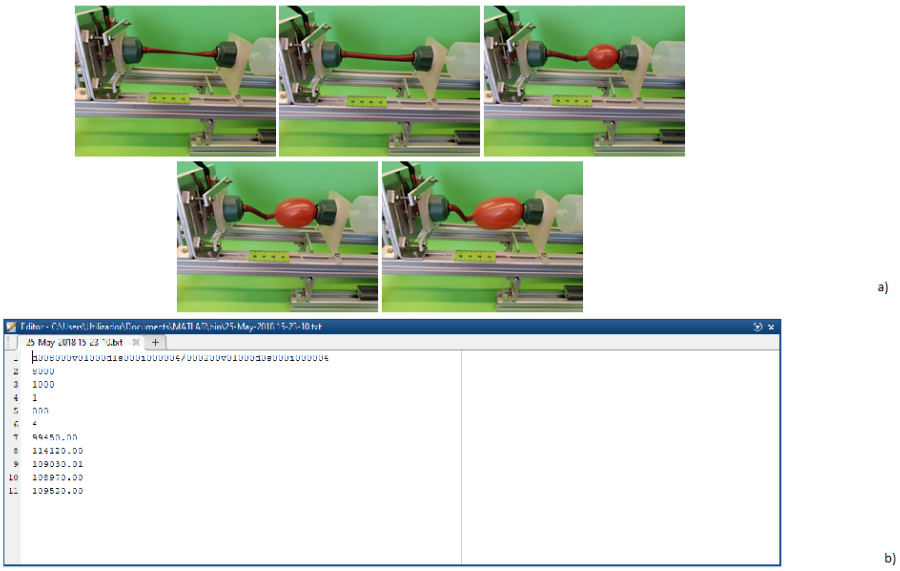

Figure 3.2: Outputs generated at the end of each task.

3.1.5 3D reconstructions

The 3D reconstructions of the object under study are performed with Fusion 360 software, from Autodesk, where the volume of fluid inside of the tubular structure is calculated from the reconstructed model (for each photo uploaded). The protocol developed to execute the reconstructions is available in chapter A, section A.2.3.3. An example is the reconstructions of the pictures of Figure 3.2 a) that are in Figure 3.3.

Figure 3.3: 3D reconstructions of the pictures of Figure 3.2 a).

3.1.6 Matlab Interface

In Figure 3.4 is represented the interface that is displayed to the user so that he can fill the parameters according to the instructions he wants to give to the device to perform a certain test.

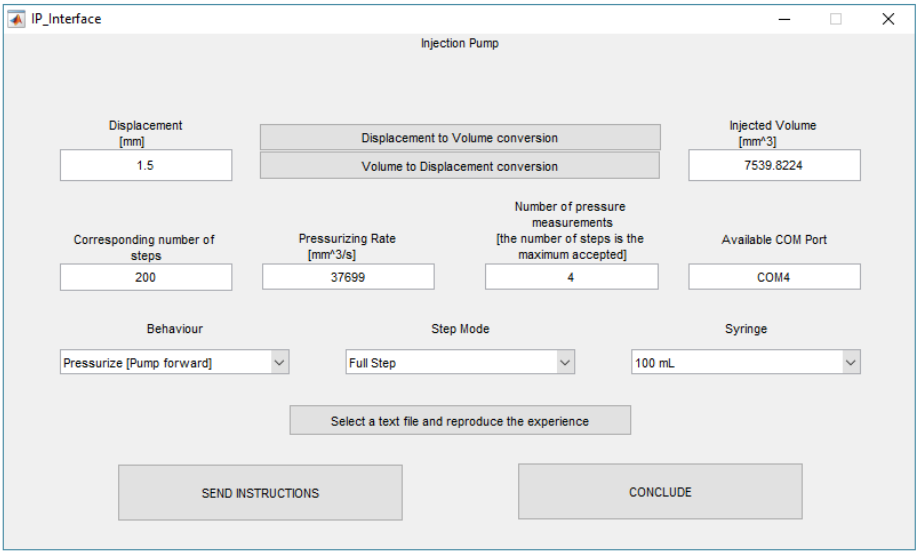

Figure 3.4: Matlab interface to control the Injection Pump device.

To perfectly control the device, the following parameters must be filled in:

Displacement: this parameter represents the displacement of the plunger of the syringe and must be written in millimeters, in the first box.

Injected volume: in this place it should be written the volume of fluid that you will be injected by the syringe into the vessel and this parameter has cubic millimeters as unities.

If only the displacement is known, it can be converted into the correspondent injected volume, pressing "Displacement to Volume conversion". Otherwise, if only the volume that will be injected is known, it can be converted into the correspondent displacement pressing the "Volume to Displacement conversion" button.

Corresponding number of steps: the value registered in this box is merely to inform what is the number of steps the motor moves depending on the required displacement. It is also useful to understand what is the maximum number of transmural pressure readings that can be perform since this maximum is equal to the number of steps that the motor will move.

Pressurizing rate: represents how many cubic millimeters of fluid are injected, per second, in the vessel and has mm^3/s as unities.
- For the 10 mL syringe, the maximum pressurizing rate is 2356.2 mm^3/s.
- For the 20 mL syringe, the maximum pressurizing rate is 9424.8 mm^3/s.
- For the 100 mL syringe, the maximum pressurizing rate is 37699 mm^3/s.

Number of readings: insert how many times the transmural pressure will be read during the displacement of the motor.

Available COM Port: write in the box in the format "COMx", being x the number of the serial port, as it is in the following example – "COM3". This information is collected when the Arduino code is sent to the board, being the procedure described in chapter A, subsection A.2.3.1.

Behaviour: select the direction of the movement, that is, the pressurization (pump forward) or depressurising (pump backward) of the object under study. This choice must be done in the available pop-up menu called "Behaviour".

Step Mode: this menu allows the user to select one of the following options for the step mode: Full, Half, Quarter, Eighth and Sixteenth step.

Syringe: choose, in the menu, which is the volume of the syringe that will be used.

This device is designed to perform more than one instruction followed. For this, all the parameters mentioned above must be filled and SEND INSTRUCTIONS button must be pressed, after the instruction is completed. After sending the task or the set of tasks desired, the CONCLUDE button should be clicked.

Select a text file and reproduce the experience

It is possible to reproduce any previous experience that has been made by this device. For this, the "Select a text file and reproduce the experience" button must be pressed and the text file gen-

erated by Matlab at the end of that experience must be selected. Matlab will read the instructions of the file, send them to Arduino and reproduce the task.

3.1.7 Relevant results from each test

Two graphs are drawn with the transmural pressure and the injected volume values measured in each test. The behaviour of the transmural pressure at different times and the behaviour of the injected volume with the transmural pressure are transposed to graphs. An example is in Figures 3.5 and 3.6, resulting these from the experience of Figures 3.2 and 3.3.

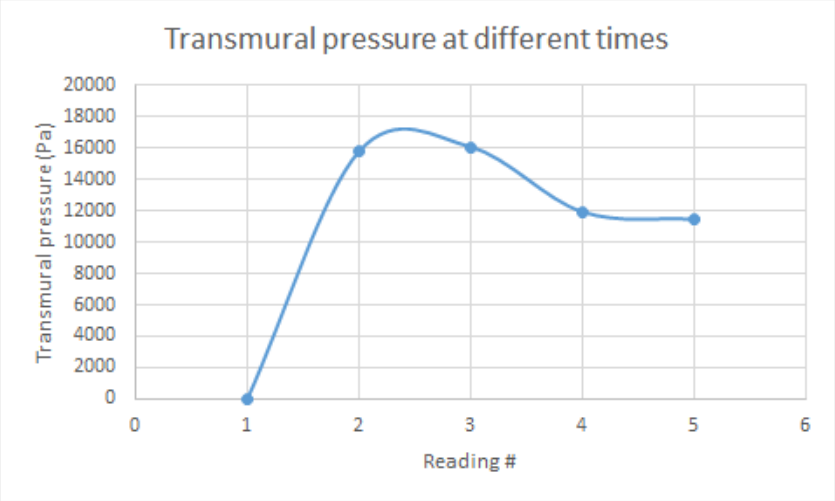

Figure 3.5: Transmural pressure at different times.

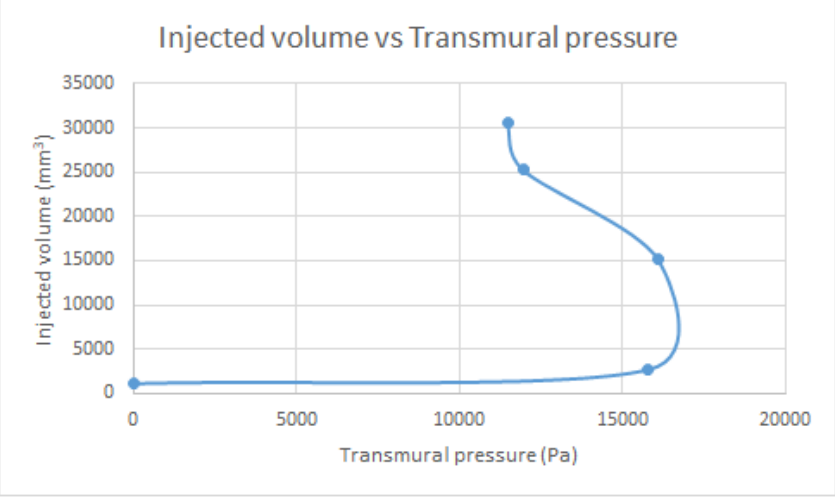

Figure 3.6: Injected volume vs Transmural pressure.

3.2 Interface upgrade

The first task performed prior joining all system components was the upgrade of the interface previously created. Figures 3.7 and 3.8 represent the two versions of the interface, before and after the improvement, respectively.

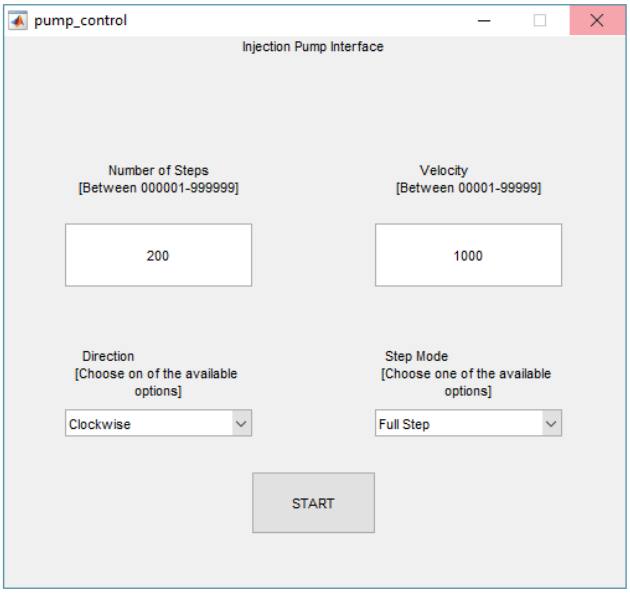

Figure 3.7: Initial Matlab-Arduino interface.

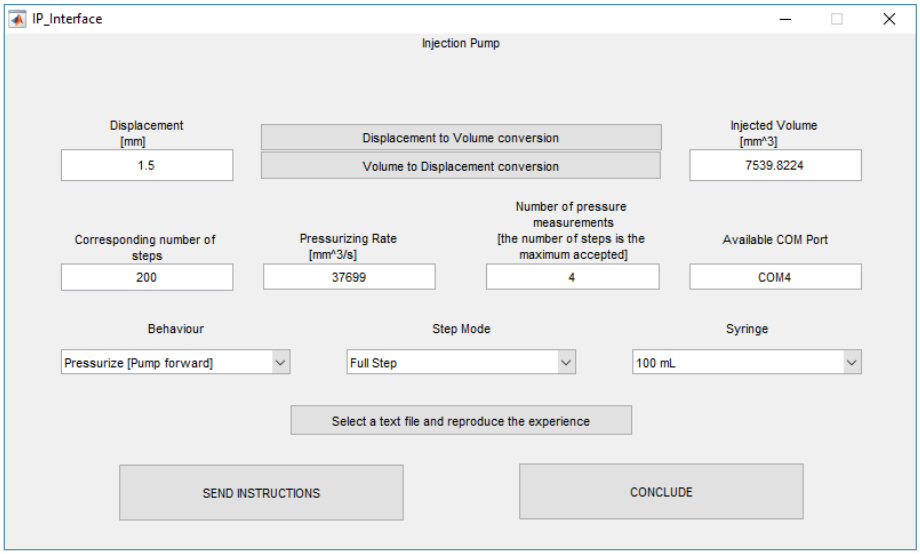

Figure 3.8: Current Matlab-Arduino interface.

In the first version (Figure 3.7), the user was asked to fulfill the parameters corresponding to the number of steps, the velocity, the direction and the step mode. However, these characteristics were related to the movement of the motor itself and not to the system. So, they were not intuitively perceptible to the user.

A conversion between the movement of the motor and the movement of the system was made. Thus, previously, the expected displacement of the motor was requested in terms of steps and now is required in terms of millimeters. In this way, the user writes the distance that wants the plunger of the syringe to move and this distance is, then, automatically converted to the number of steps the motor has to give. This step made it easier and more noticeable. The user does not have to know anything more than the displacement that wants to the plunger of the syringe to move.

If the user does not know how many millimeters that wants the plunger to move but only knows the amount of fluid to be injected, he can write the value of the injected volume and convert it to displacement by using the "Volume to Displacement conversion" button. The opposite, "Displacement to Volume conversion" is available too.

Similarly to the displacement, the velocity was previously requested in terms of number of steps per second and now is asked for the user to write the pressurizing rate, that is, how many cubic millimeters of fluid wants to be injected into the specimen under study per second. Again, the conversion turned this task easier.

Three new parameters have been added to the interface: the number of steps, the number of pressure measurements and the available COM port. The first is merely informative and is used for the user to confirm if the number of steps that the motor will take is greater than the number of pressure readings during the work. The second is used for the user to register how many transmural pressure records he wishes to be carried out during the experimental work. In last parameter, the user has to mention which serial port is available to establish the connection between the Arduino and Matlab.

The Direction pop-up menu was replaced by Behaviour menu, which concerns the direction of the behaviour of the task. That is, if the plunger of the syringe moves forward or backward and, thus, pressurize or depressurize the tissue under study. Previously, the user would have to choose if the direction was Clockwise or Counterclockwise, which had no meaning for him and was directly related to the motor and not with the device. The Step Mode popup menu remains the same.

The Syringe menu is a new addition. In this menu, different volume values are found for the syringe. Thus, conversions can be made directly, with the physical dimensions of each instrument directly associated.

New functions have been added to the device. Now, it is possible to reproduce previous experiences, using the text file generated by Matlab at the end of this task. The user only has to upload this document via the "Select a text file and reproduce the experience" button. Another possible operation is to send different instructions at once, which will be executed one after the other. These functionalities were not available in the first version of the interface.

The START button was replaced by the "SEND INSTRUCTIONS" and "CONCLUDE" but-

tons. The first must be used every time someone wants to send one instruction and the last must be used when the user wants to start the execution of the desired task/set of tasks.

As explained above, with all the modifications made, the interface has become easier to use and the requested parameters more noticeable. The new functionalities have made the device more usable and possible to reproduce of previous experiments.

3.3 Clamp of the tubular structures

An innovative, and never seen before, way was used to attach the object under study to the Injection Pump device. The method used in the apparatus developed is in Figure 3.9.

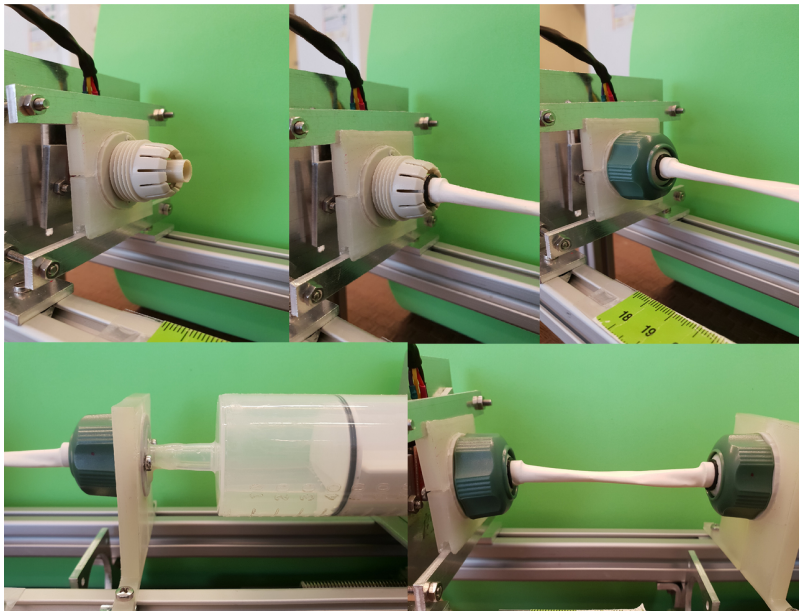

Figure 3.9: Method used to clamp the specimen.

Two hose connections were cut and adapted so that their inner tubes could be introduced into the extremities of the specimen. The extremities of the object were inserted between the inner tube and the tightening teeth. After that, the screw thread was introduced and tight to hold the structure and to keep it suspended. This bold mechanism is a safe and effective way to hold the structure and to prevent leakage of fluid during the pressurizing process.

Chapter 4

Methodology

In this chapter is presented the methodology followed in the execution of the experimental tests. First, are presented the steps taken in carrying out the balloon tests and then all the preparation necessary for performing the test in the organic material.

4.1 Preliminary tests

In order to prepare the device for performing tests in organic structures and in an attempt to prevent possible failures, inflation tests were performed in long balloons, whose shape is very similar to that of the blood vessels.

Three different types of tests were performed: having air, water or saline solution as the pressurizing fluid. For these three tests, the methodology followed was the same, being the unique difference the fluid that was inside the syringe.

The first step was to fill the syringe with liquid (in the case air is not used). After that, the long balloon was mounted between the two hose connections, where one was attached to the syringe and the other to the pressure sensor (Figure 4.1).

Figure 4.1: Balloon assembly.

The balloon was attached to the hose connections using a O-ring and tight with the screw thread, as in Figure 4.2.

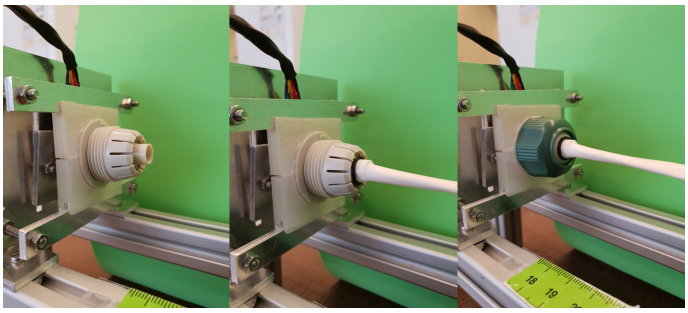

Figure 4.2: Attachment of the balloon to the hose connections.

After these steps were completed, different tests were executed and they are explained in detail in chapter 5.

The methodology for the preliminary tests is very basic, since it is not necessary to apply any treatment to the balloon. The generated photos were uploaded in the Fusion 360 software and the 3D reconstruction of the balloon was performed, as explained in chapter A. The values of the injected volume of fluid inside the balloon were measured and these values, along with transmural pressure values, were used to draw two graphs, Transmural pressure at different times and Injected volume vs Transmural pressure.

4.2 Tests with organic structures

4.2.1 Specimen preparation

A piece of aorta from one approximately seven-month-old pig was obtained from a local vendor and stored in saline solution at 5°C until testing, since the test was not performed immediately after harvest.

The 90 mm specimen was obtained by making an axial incision along the proximal side of the aorta. All aortic branches were kept intact and these were ligated with suture thread.

A sensitive condom was placed inside the vessel to prevent possible leakage of pressurizing fluid. The introduction of the condom does not influence the resistance of the aorta to inflation, since it is not resistant to deformation and, therefore, the deformation of the vessel is due to the pressure exerted by the fluid on the walls of the artery.

After completing this procedure, the artery was connected to the hose connection, as in Figure 4.3.

Figure 4.3: Piece of aorta with 90 mm of length.

4.2.2 Test protocol

The reference length at zero transmural pressure was recorded. The inflation was performed by pressurizing the specimen at a pressurizing rate of 18850 mm^3/s, over a wide transmural pressure range from 0 to 13770 Pa (0-103 mm Hg), at room temperature.

Images of the specimen were recorded simultaneously with transmural pressure measurements. These images were uploaded in the Fusion 360 software and the 3D reconstruction of the artery was performed. With the values of the injected volume of saline solution and the transmural pressure values, two graphs were designed - Transmural pressure at different times and Injected volume vs Transmural pressure.

Chapter 5

Results and discussion

This chapter contains the results obtained in this dissertation and their discussion. First, different tests were performed to long balloons, in order to evaluate the behaviour of the Injection Pump device. So, the performance of the device regarding the ability to perform different displacements taking into consideration the same pressurizing rate, and to perform the same displacement at different pressurizing rates as well as the use of different pressurizing fluids was evaluated. After that, a test was performed to porcine aortic tissue.

5.1 Preliminary tests

The preliminary tests made in the developed device were performed to a long balloon, which was used as tubular structure. These tests were performed as a way of preparing the assays in organic tissues.

In order to infer the consistency of the results and thus the accuracy of the Injection Pump device, three assays were performed for each test and the results are presented as mean value $\pm$ standard deviation.

5.1.1 Long balloon inflated with air

The first test done, with the device, was the filling of a long balloon with air. In this way, the device was required to move the plunger of the syringe 60 mm, in the direction of pressurizing, with a pressurizing rate of 18850 mm^3/s, full step mode and to perform 4 readings of the transmural pressure value inside the balloon, during the task (Test 1).

The outputs of the experience were 5 photographs, one of the initial moment (when there was no pressure applied to the balloon) and the remaining 4 taken at the moment of measuring the transmural pressure value, and a text file with the requested instructions and the transmural pressure values measured.

At the end, the generated photos were uploaded in the Fusion 360 software and the 3D reconstruction of the balloon was performed, as explained in chapter A, section A.2.3.3. The values of

the injected volume of air inside the balloon were measured and these values, along with transmural pressure values, were used to draw two graphs, Transmural pressure at different times and Injected volume vs Transmural pressure. The photographs and their 3D reconstructions are represented in Figures 5.1-5.5.

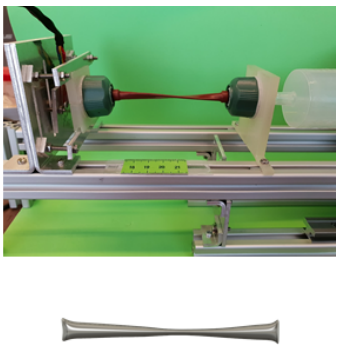

Figure 5.1: Balloon deformation state at the initial time (Test 1).

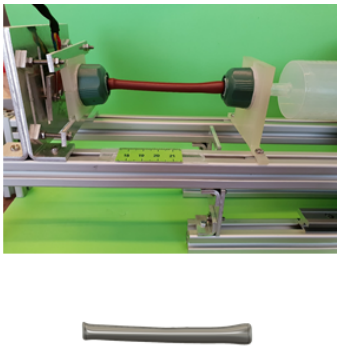

Figure 5.2: Balloon deformation state at the second transmural pressure measurement (Test 1).

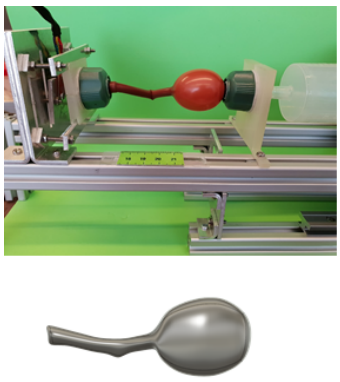

Figure 5.3: Balloon deformation state at the third transmural pressure measurement (Test 1).

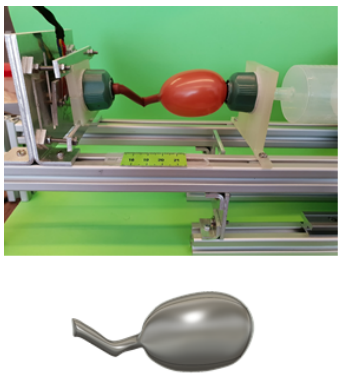

Figure 5.4: Balloon deformation state at the fourth transmural pressure measurement (Test 1).

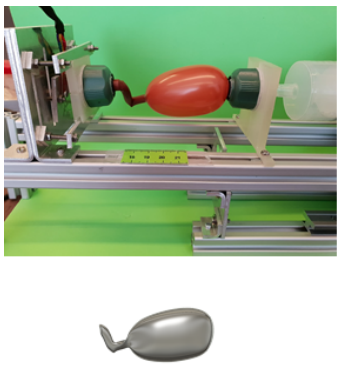

Figure 5.5: Balloon deformation state at the fifth transmural pressure measurement (Test 1).

The volume of air inside the balloon and the value of the transmural pressure at each moment are shown in the Table 5.1 and the graphs created with these values are presented in Figures 5.6 and 5.7.

Table 5.1: Transmural pressure and injected volume values (Test 1)

Reading number	Transmural pressure (Pa)	Injected volume (mm^3)
1	0.00±0.00	1154.148±5.853
2	15636.67±265.50	3054.641±70.168
3	11303.34±1617.10	15727.333±578.205
4	10796.67±1040.05	23660.000±808.125
5	10890.00±1122.71	34510.667±1775.331

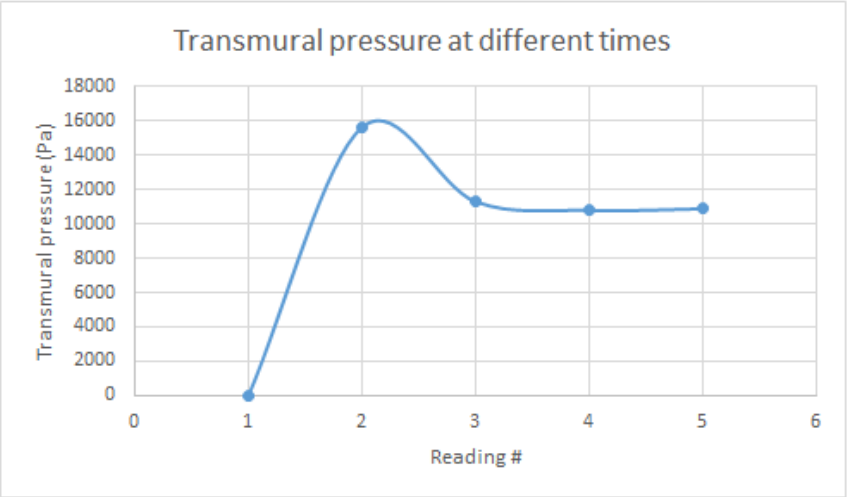

Figure 5.6: Transmural pressure at different times (Test 1).

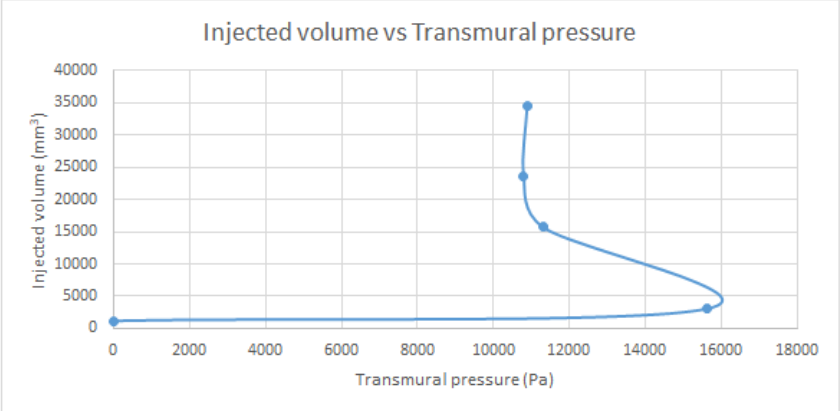

Figure 5.7: Injected volume vs Transmural pressure (Test 1).

Observing Transmural pressure over time (Figure 5.6), it is possible to understand that the first value of transmural pressure is the smallest of the set, once it was recorded at the initial moment, when no pressure was being applied to the balloon. This value was 0.00 Pa, which is as expected, since the transmural pressure is given by the difference of the pressure inside the balloon and the pressure outside of it (atmospheric pressure) and, at the initial moment, the pressure inside the balloon is the atmospheric pressure.

From the initial value, the pressure increased, until the third value collected, where a decrease of this value is observed. This phenomenon is due to the fact that the value of resistance of the balloon's material has been exceeded. That is, the pressure of the injected air exceeded the yield pressure of the balloon's walls thus being the force required for this to fill smaller and, therefore, the pressure inside the balloon has decreased. From the third record, the pressure started to increase again but, this time, with small increments.

Through graph Injected volume vs Transmural pressure (Figure 5.7) it is possible to conclude that the volume of air inside the balloon at the initial moment was 1154.148 mm^3 and that has increased over time, as expected. However, until the value of the resistance of the balloon being exceeded, the volume of air injected was very small. From that moment, the volume increased from 3054.641 mm^3 to 34510.667 mm^3. Looking at Figure 5.5, it is clearly noticeable that the volume of air inside the balloon is much higher than that observed in the other photographs.

The mean standard deviation of the transmural pressure values was about 9%, which is a little bit bigger than the acceptable value - 5% - suggesting that the measurements were not made with great accuracy, and for the injected volume was about 3%, which is a very good value.

In order to compare the effect of the velocity in the process of filling the balloon, another test was executed (Test 2). This time, the required displacement was the same as the previous one (Test 1) but the pressurizing rate was twice as great. So, the task was to move the plunger of the syringe 60 mm, with a pressurizing rate of 37699 mm^3/s and the remaining parameters (direction and step mode) were maintained. The recorded photos and their 3D reconstructions are represented in Figures 5.8-5.12.

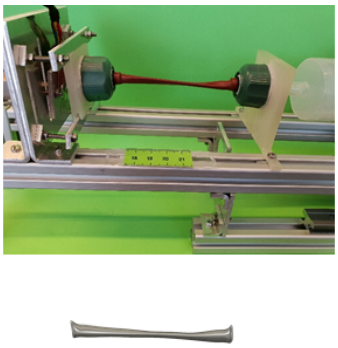

Figure 5.8: Balloon deformation state at the initial time (Test 2).

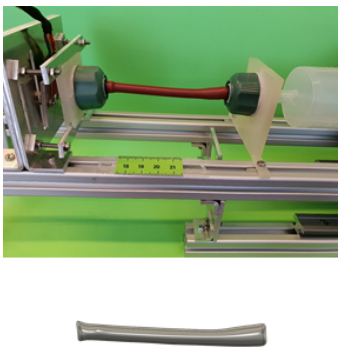

Figure 5.9: Balloon deformation state at the second transmural pressure measurement (Test 2).

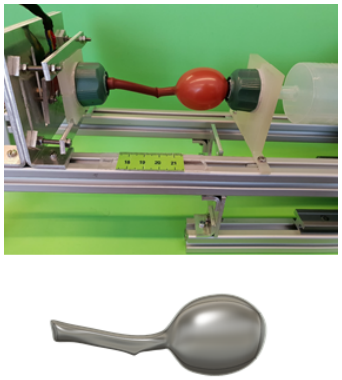

Figure 5.10: Balloon deformation state at the third transmural pressure measurement (Test 2).

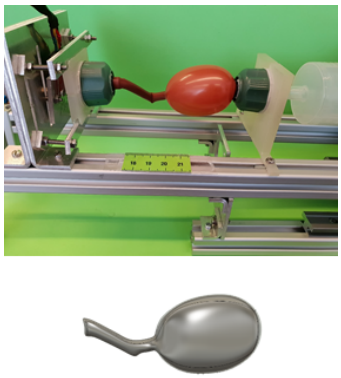

Figure 5.11: Balloon deformation state at the fourth transmural pressure measurement (Test 2).

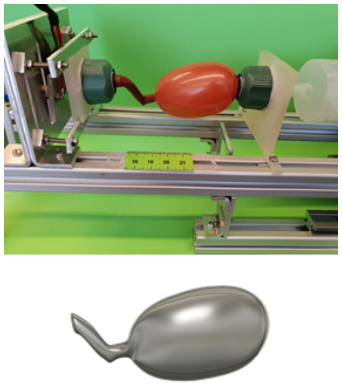

Figure 5.12: Balloon deformation state at the fifth transmural pressure measurement (Test 2).

In Table 5.2 and in the graphs of Figures 5.13 and 5.14, are the values of the transmural pressure and injected volume during the task, at different moments (when the transmural pressure value is collected).

Table 5.2: Transmural pressure and injected volume values (Test 2)

Reading number	Transmural pressure (Pa)	Injected volume (mm^3)
1	0.00±0.00	1110.083±62.827
2	15805.00±1135.00	2698.090±52.167
3	16090.01±6510.00	15144.000±334.000
4	11945.00±2425.00	25268.000±372.000
5	11470.00±1400.00	30505.000±55.000

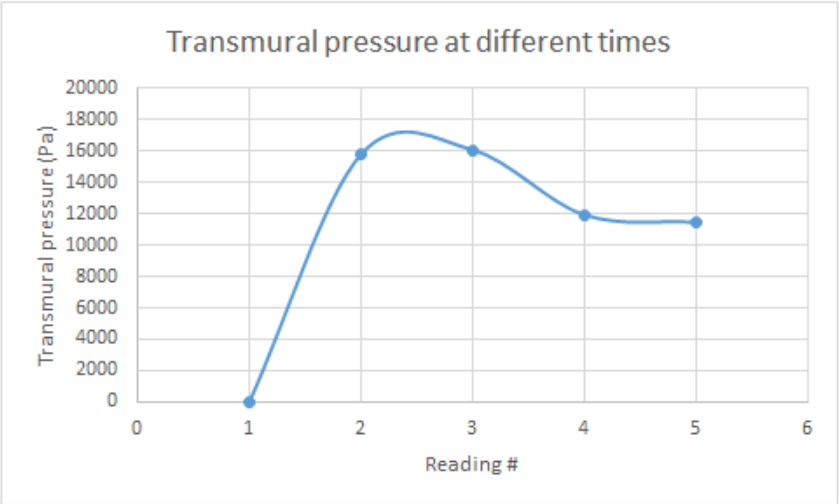

Figure 5.13: Transmural pressure at different times (Test 2).

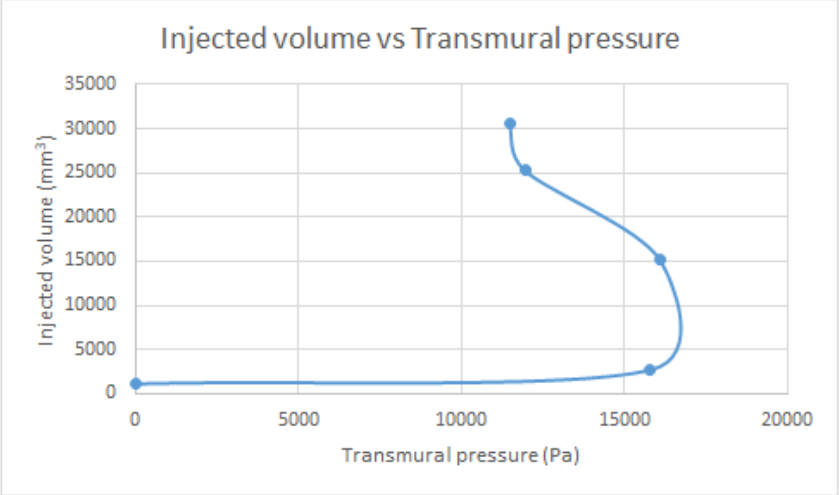

Figure 5.14: Injected volume vs Transmural pressure (Test 2).

Once again, the transmural pressure at the initial moment was 0.00 Pa and equal to the first measurement of the previous test (Test 1). Until the second pressure value was collected, it increased and then began to decrease, as can be observed in graph Transmural pressure over time (Figure 5.13). This diminishment of the transmural pressure is due to the resistance of the balloon's material have been exceed and, so, it is not necessary even pressure value to fill the balloon with the same amount of air.

Looking at graph Injected Volume vs Transmural pressure (Figure 5.14), and as it is expected, the injected volume increases with the transmural pressure. Although, the amount of volume is higher after the transmural pressure starts to decrease because with the same transmural pressure, a higher volume of air is injected in the balloon. Comparing the values of transmural pressure of

both tests (Table 5.1 and 5.2), it is possible to conclude that the pressurizing rate has no influence in the process of filling the balloon, since the initial (P=0.00 Pa, V=1154.148 mm^3; P=0.00 Pa, V=1110.083 mm^3) and final (P=10890.00 Pa, V=34510.667 mm^3; P=11470.00 Pa, V=30505.000 mm^3) values of transmural pressure and volume are very similar.

Thus, different pressurizing rates in the process of filling the balloon with the same quantity of air (being the displacement of the plunger of the syringe the same in both tests), has no significant differences. The only difference is the time that the task takes, that is, a higher pressurizing rate takes less time to fulfill the balloon.

In this test, the mean standard deviation for the transmural pressure values was about 20%, which we may consider a very high value. However, this parameter for the injected volume values was about 2.3%.

In the sense of studying the performance of the device regarding the ability to perform different displacements taking into consideration the same pressurizing rate, two different tests were executed. In the first test (Test 3), the behavior of the device was evaluated in the case of half the displacement carried out up to now but with an equal pressurizing rate. In that way, the plunger of the syringe was moved 30 mm, at a pressurizing rate of 18850 mm^3/s, and to measure the transmural pressure five times. The remaining values were maintained. The photos generated and their reconstructions are in Figures 5.15-5.20. The values obtained from the task are represented in Figures 5.21 and 5.22 and Table 5.3.

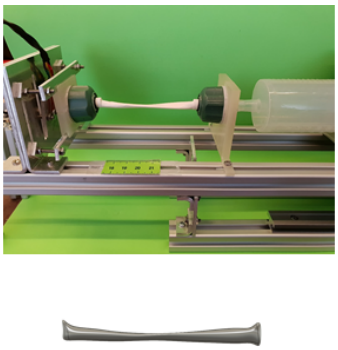

Figure 5.15: Balloon deformation state at the initial time (Test 3).

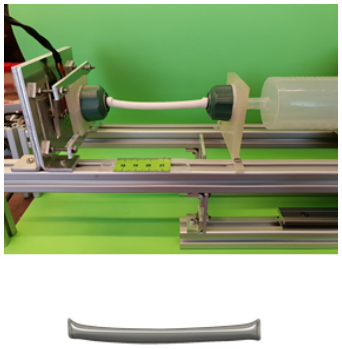

Figure 5.16: Balloon deformation state at the second transmural pressure measurement (Test 3).

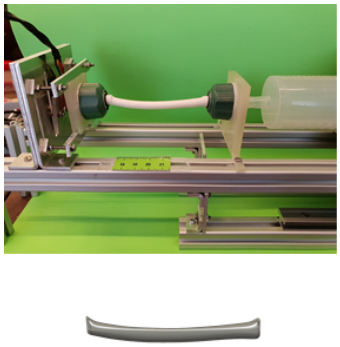

Figure 5.17: Balloon deformation state at the third transmural pressure measurement (Test 3).

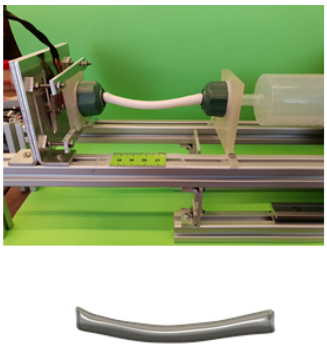

Figure 5.18: Balloon deformation state at the fourth transmural pressure measurement (Test 3).

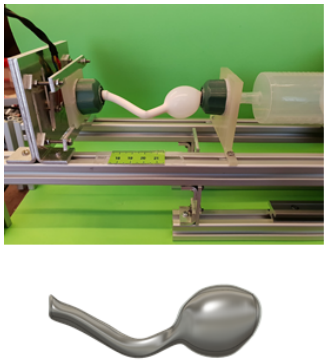

Figure 5.19: Balloon deformation state at the fifth transmural pressure measurement (Test 3).

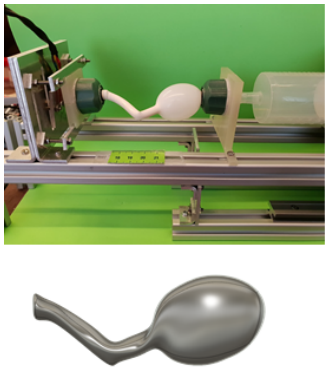

Figure 5.20: Balloon deformation state at the sixth transmural pressure measurement (Test 3).

Table 5.3: Transmural pressure and injected volume values (Test 3)

Reading number	Transmural pressure (Pa)	Injected volume (mm^3)
1	0.00±0.00	1358.952±27.963
2	5980.00±150.14	1744.311±65.789
3	12790.00±857.52	2096.478±45.321
4	19360.00±1063.78	2724.826±104.128
5	12190.00±733.78	12380.000±647.625
6	11580.00±789.63	18810.000±896.201

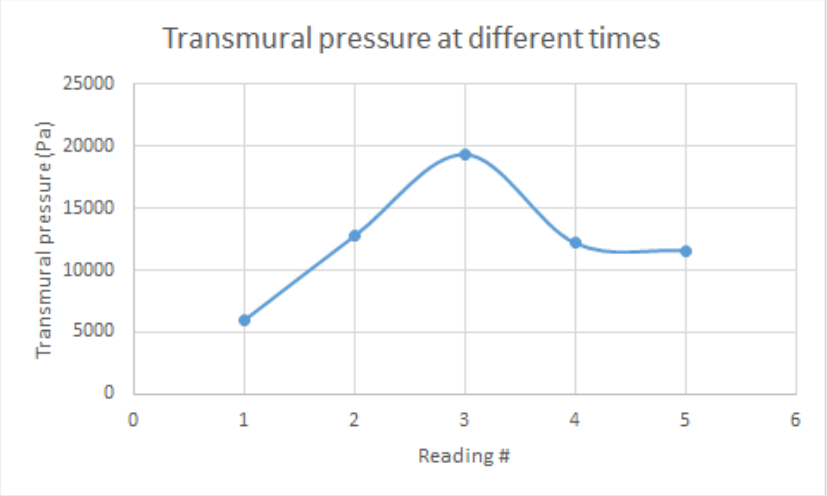

Figure 5.21: Transmural pressure at different times (Test 3).

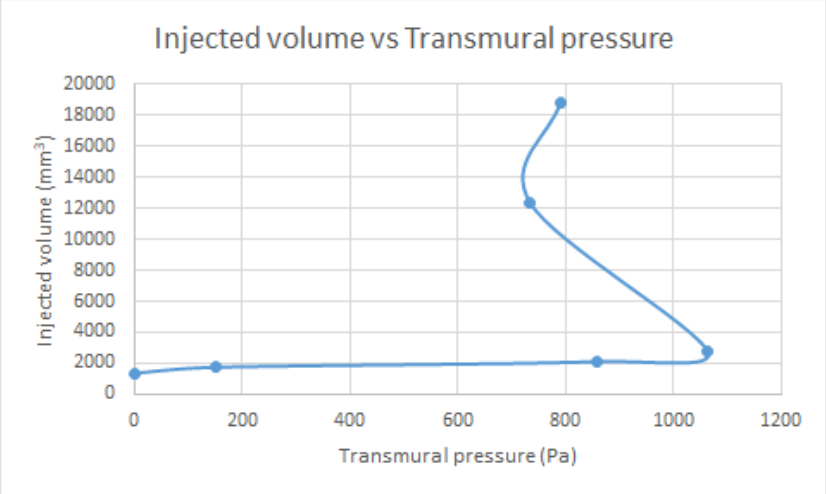

Figure 5.22: Injected volume vs Transmural pressure (Test 3).

Through the observation of Figure 5.21 (Transmural pressure over time), it is possible to conclude that transmural pressure increases until the moment when the balloon strength was exceeded. From that moment, the transmural pressure decreases and then increases again but at very small intervals. With the injected volume being taken into account, the behavior already described above is repeated, that is, the volume increases very little until the expiration of the resistance of the balloon and thereafter increases considerably, as can be confirmed in graph Injected volume vs Transmural pressure (Figure 5.22).

Comparing the results of the tests that were carried out with the same velocity but different displacements (Tables 5.1 and 5.3), it can be seen that the transmural pressure values collected are very similar, being the final values P=10890.00 Pa (Test 1) and P=11580.00 Pa (Test 3). However,

looking at the injected volume values, these are quite difference, one being roughly half of the other [V=34510.667 mm^3 (Test 1); V=18810.000 mm^3 (Test 3)].

The transmural pressure had 5.4% as mean value of the standard deviation and the injected volume had 3.6% as value for this parameter. As both are equal or lower than 5%, we may consider that the measurements are very consistent.

In the second test (Test 4) the performance of the device was evaluated for the same pressurizing rate but for a quarter of the initial displacement, that is, a pressurizing rate of pressurizing rate=18850 mm^3/s and a syringe plunger displacement of 15 mm. The images generated and their 3D reconstructions are presented in Figures 5.23-5.27 and the values in the Table 5.4 and in the graphs of Figures 5.28 and 5.29.

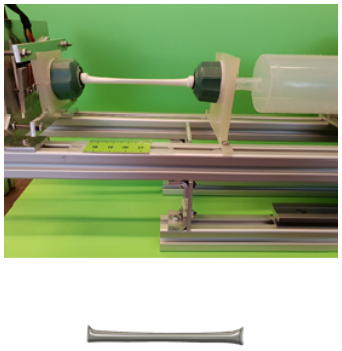

Figure 5.23: Balloon deformation state at the initial time (Test 4).

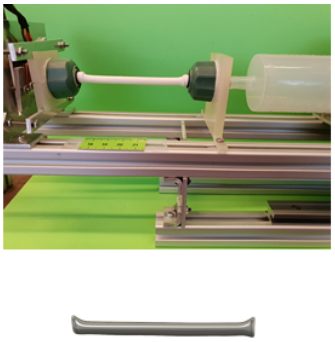

Figure 5.24: Balloon deformation state at the second transmural pressure measurement (Test 4).

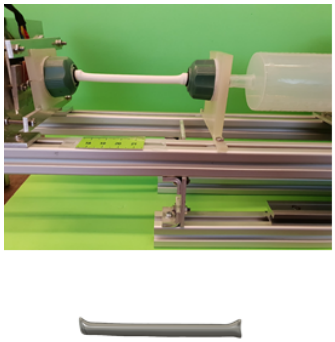

Figure 5.25: Balloon deformation state at the third transmural pressure measurement (Test 4).

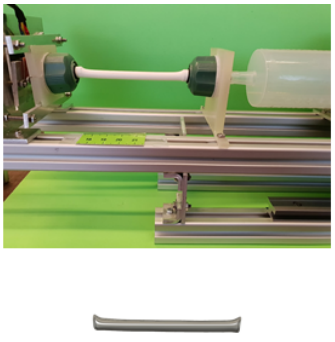

Figure 5.26: Balloon deformation state at the fourth transmural pressure measurement (Test 4).

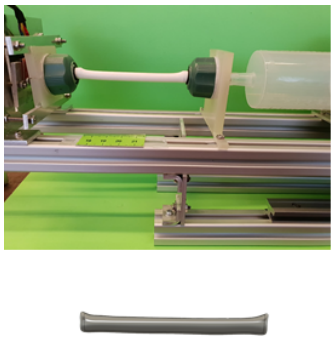

Figure 5.27: Balloon deformation state at the fifth transmural pressure measurement (Test 4).

Table 5.4: Transmural pressure and injected volume values (Test 4)

Reading number	Transmural pressure (Pa)	Injected volume (mm^3)
1	0.00±0.00	1076.115±39.121
2	3525.00±225.00	1646.368±24.173
3	7645.00±175.00	1822.902±2.552
4	11900.00±190.00	1901.371±2.140
5	15595.00±325.00	2024.994±0.648

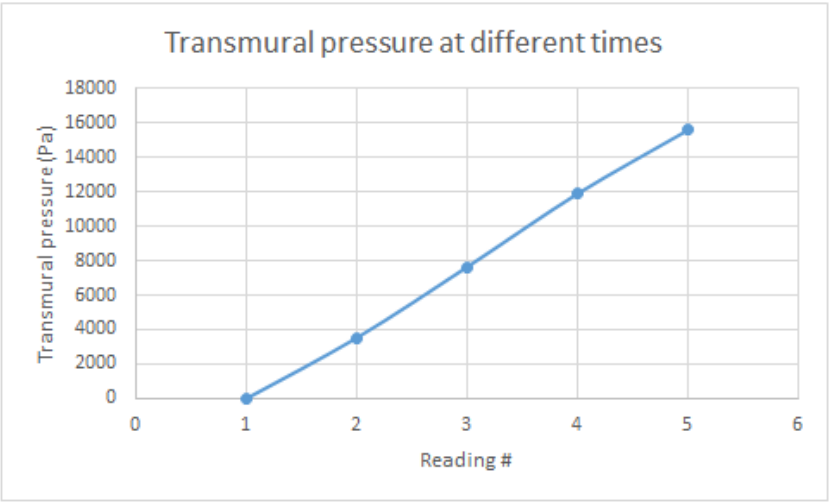

Figure 5.28: Transmural pressure at different times (Test 4).

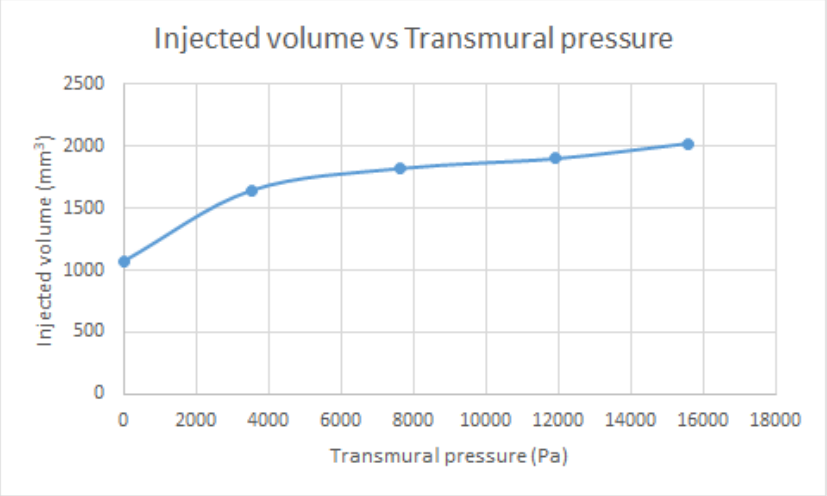

Figure 5.29: Injected volume vs Transmural pressure (Test 4).

Through the graph Transmural pressure over time (Figure 5.28) and the last picture of Figure 5.27, it is possible to see that the value of the balloon strength was not exceeded as the transmural pressure increased linearly at light intervals from the beginning to the end of the task. The same happened with the volume of air injected (Injected volume vs Transmural pressure - Figure 5.8), which was increasing slightly with the pressure.

By comparing these results with those of the first experiment (Tables 5.1 and 5.4), taking the displacement by a quarter of the initial displacement, it can be assumed that the transmural pressure values over the duration of the experiment are very similar, with the initial values of P=0.00 Pa (Test 1) and P=0.00 Pa (Test 4) and final values of P=10890.00 Pa (Test 1) and P=15920.00 Pa (Test 4). The injected volume throughout the experiment (Injected volume vs Transmural pressure - Figure 5.29) is very different for the two tests, with the final values of V= 34510.667 mm^3 (Test 1) and V= 2024.346 mm^3 (Test 4).

The results of these tests are as expected, since the volume injected depends on the displacement of the plunger of the syringe, as can be evidenced by the expression $v = \pi r^2 h$, where r is the radius of the syringe and h is the displacement of the plunger of the syringe.

3% and 1% were the mean standard deviation values for the transmural pressure and injected volume values, respectively, which are very low values and that means a high level of consistency between the measurements.

5.1.2 Long balloon inflated with water

In order to evaluate the behaviour of the balloon when different fluids are used, another set of tests were performed but this time with water and the results were compared with the results of the tests using air.

In the first test (Test 5), the device was required to move the plunger of the syringe 60 mm,

in the direction of pressurizing, with a pressurizing rate of 18850 mm^3/s, full step mode and to perform 4 readings of the transmural pressure value inside the balloon, during the task. The photographs resulting of the test are in the Figures 5.30-5.34 and the values collected are expressed in Table 5 and in the graphs of Figures 5.35 and 5.36.

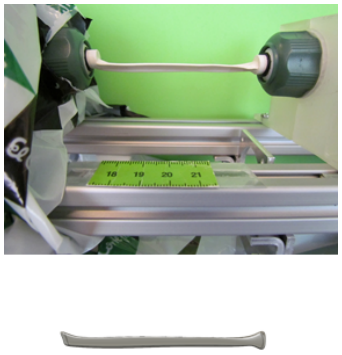

Figure 5.30: Balloon deformation state at the initial time (Test 5).

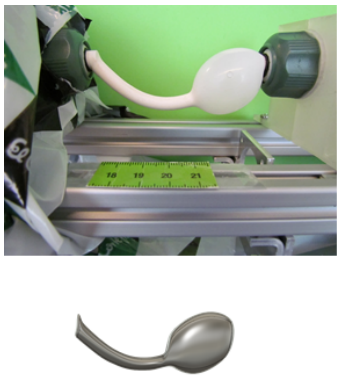

Figure 5.31: Balloon deformation state at the second transmural pressure measurement (Test 5).

Figure 5.32: Balloon deformation state at the third transmural pressure measurement (Test 5).

Figure 5.33: Balloon deformation state at the fourth transmural pressure measurement (Test 5).

Figure 5.34: Balloon deformation state at the fifth transmural pressure measurement (Test 5).

Table 5.5: Transmural pressure and injected volume values (Test 5)

Reading number	Transmural pressure (Pa)	Injected volume (mm^3)
1	0.00±0.00	394.575±39.121
2	13240.00±195.00	9272.868±24.173
3	12720.00±175.00	22750.000±26.552
4	13300.00±190.00	34060.000±42.140
5	13670.01±325.00	52350.000±64.800

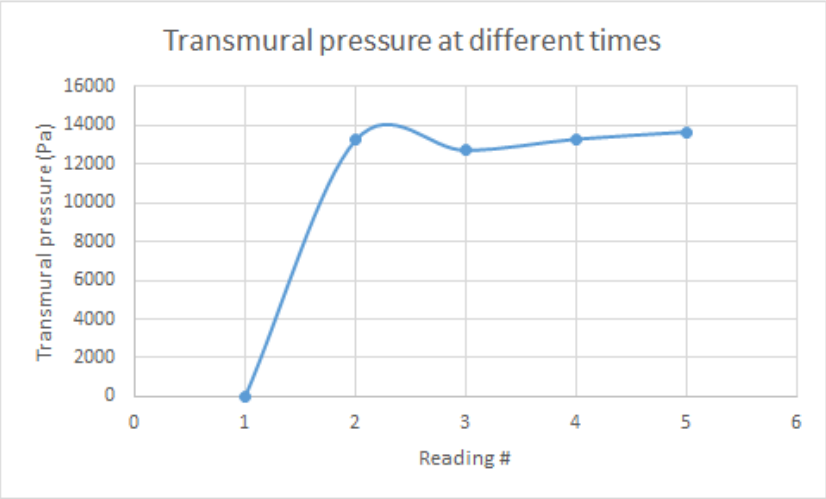

Figure 5.35: Transmural pressure at different times (Test 5).

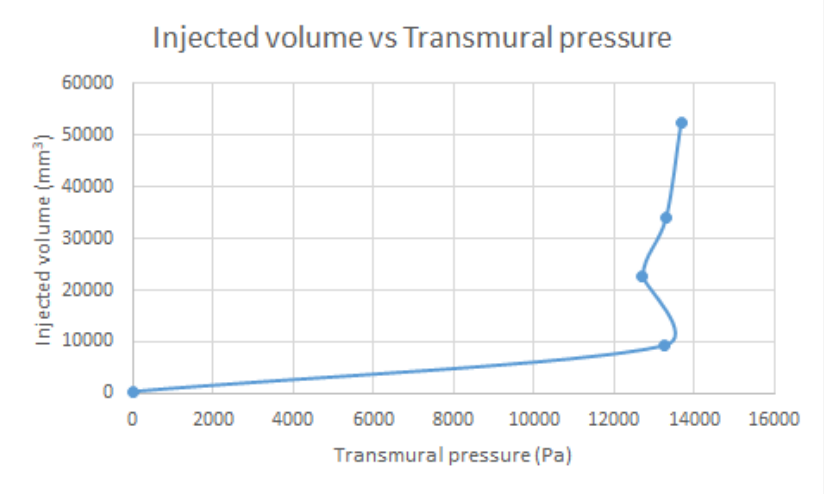

Figure 5.36: Injected volume vs Transmural pressure (Test 5).

Through graph Transmural pressure over time (Figure 5.35), it is possible to understand that the transmural pressure starts with the value of zero (when the difference of pressure between the balloon's wall is null), that is, when there is no pressure applied to the balloon, just as in the case of the fluid being air (Test 1). With time, the transmural pressure increases until it exceeds the value of the resistance of the balloon. After that, the transmural pressure decreases but soon increases again but at smaller intervals.

The injected volume follows the opposite behaviour, that is, increases in small intervals until the resistance of the balloon is overcome and after that moment increases in more considerable intervals (Injected volume vs Transmural pressure – Figure 5.36).

At the final of the task, the transmural pressure took the final value of 13670.01 Pa and the injected volume took the value of 52350.000 mm^3 (Table 5.5).

Comparing the results of this test with the results of the same test made with air (Tables 5.1 and 5.5), it is noticeable that the final injected volume of the test made with water is substantially greater than that achieved with air.

It can be assumed that the measurements were accurate, since the mean standard deviation for the transmural pressure values was 2.8% and for the injected volume values was 2.4%.

The test was repeated for half the displacement of the previous test (Test 6), being the remaining values the same (displacement=30mm, pressurizing rate=18850 mm^3/s, full step mode, 4 readings of the transmural pressure). The resulting photos and their reconstructions are shown in Figures 5.37-5.41 and the values of the transmural pressure and the injected volume are described in Table 5.6 and in the graphs of Figures 5.42 and 5.43.

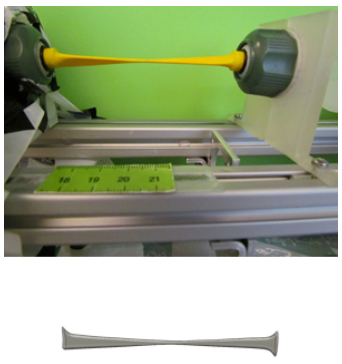

Figure 5.37: Balloon deformation state at the initial time (Test 6).

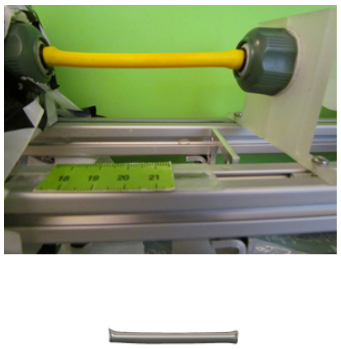

Figure 5.38: Balloon deformation state at the second transmural pressure measurement (Test 6).

Figure 5.39: Balloon deformation state at the third transmural pressure measurement (Test 6).

Figure 5.40: Balloon deformation state at the fourth transmural pressure measurement (Test 6).

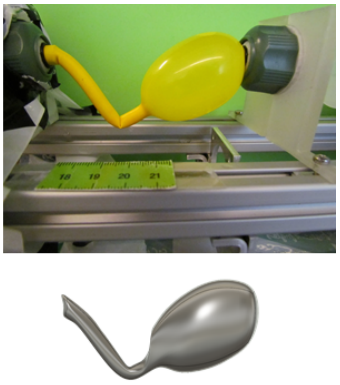

Figure 5.41: Balloon deformation state at the fifth transmural pressure measurement (Test 6).

Table 5.6: Transmural pressure and injected volume values (Test 6)

Reading number	Transmural pressure (Pa)	Injected volume (mm^3)
1	0.00±0.00	343.005±12.445
2	14650.00±4051.72	1557.502±102.791
3	10673.34±1871.47	9552.818±59.182
4	10216.67±1798.42	15864.000±867.912
5	10366.67±1826.70	20564.138±700.544

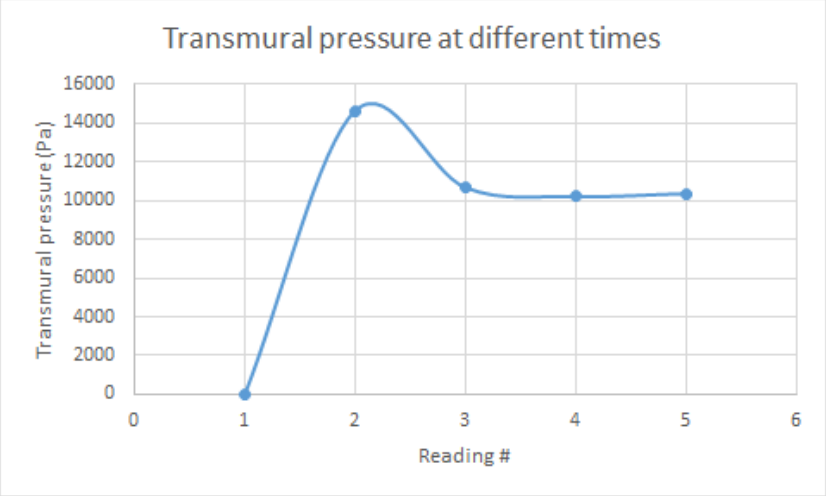

Figure 5.42: Transmural pressure at different times (Test 6).

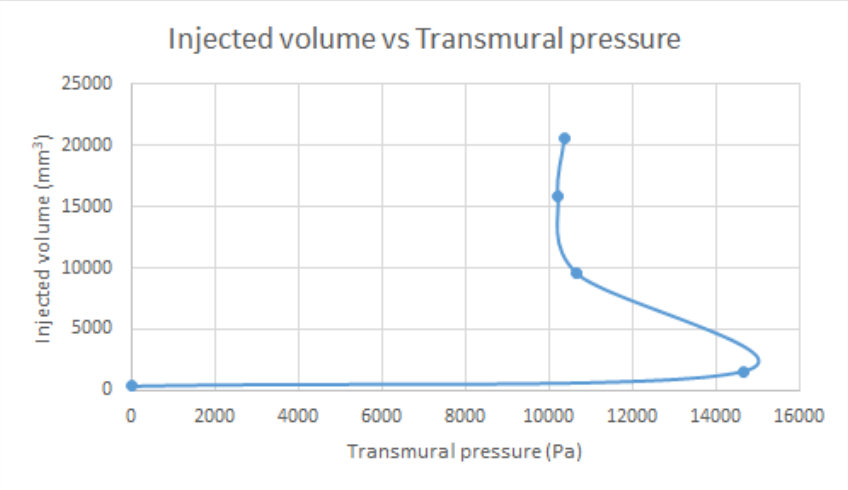

Figure 5.43: Injected volume vs Transmural pressure (Test 6).

Observing Figures 5.42 and 5.43, it is possible to see that the transmural pressure values and the injected volume values take the same behavior as the previous test (Test 5). Despite the values of the transmural pressure were very similar in both tests, the final value of the injected volume were very different, taking the value of 52350.00 mm^3 for Test 5 and 20564.138 mm^3 for Test 6. This event is in line with what is expected, since the injected volume depends on the displacement and, therefore, a smaller displacement leads to a lower fluid injection.

The measurements of the transmural pressure were a bit dissenting, since the mean standard deviation was about 20%. In contrast, the same parameter for the injected volume values was about 4%, which is a very good value.

The last test performed using water as fluid (Test 7) was executed with the goal to analyze the behaviour of the device when equal displacements are carried out at different pressurizing rates. In that way, the device was required to move the plunger of the syringe 60 mm, in the direction of pressurizing, with a pressurizing rate of 37699 mm^3/s (twice as high as in the first test), full step mode and to perform 4 readings of the transmural pressure value, during the experiment.

The collected pictures and their 3D reconstructions are in Figures 5.44-5.48 and the values of the transmural pressure and the injected volume can be found in Table 5.7 and in Figures 5.49 and 5.50.

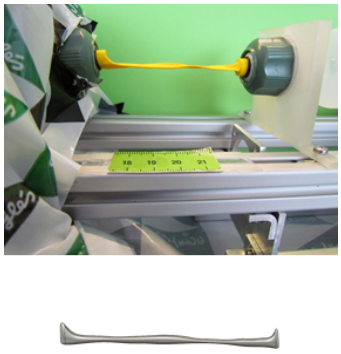

Figure 5.44: Balloon deformation state at the initial time (Test 7).

Figure 5.45: Balloon deformation state at the second transmural pressure measurement (Test 7).

Figure 5.46: Balloon deformation state at the third transmural pressure measurement (Test 7).

Figure 5.47: Balloon deformation state at the fourth transmural pressure measurement (Test 7).

Figure 5.48: Balloon deformation state at the fifth transmural pressure measurement (Test 7).

Table 5.7: Transmural pressure and injected volume values (Test 7)

Reading number	Transmural pressure (Pa)	Injected volume (mm^3)
1	0.00±0.00	172.588±4.741
2	16470.00±541.23	3162.172±245.612
3	14190.00±747.85	17680.000±1063.512
4	14770.00±395.45	29100.000±741.852
5	15620.01±79.47	43510.000±1245.745

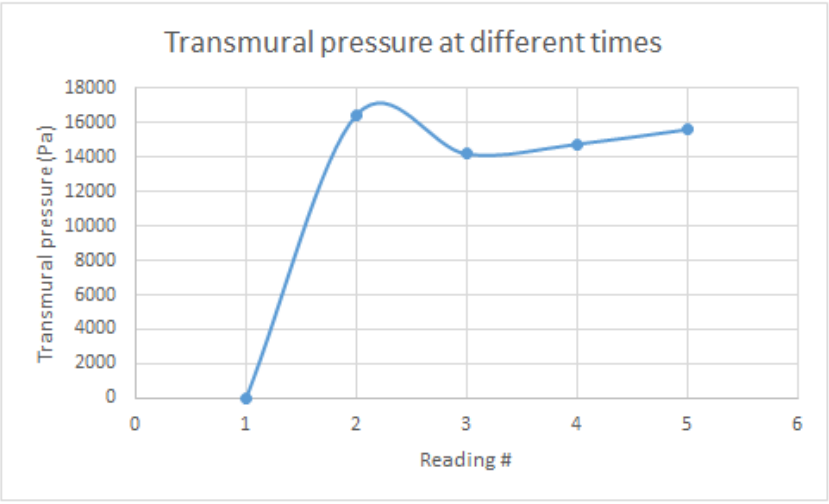

Figure 5.49: Transmural pressure at different times (Test 7).

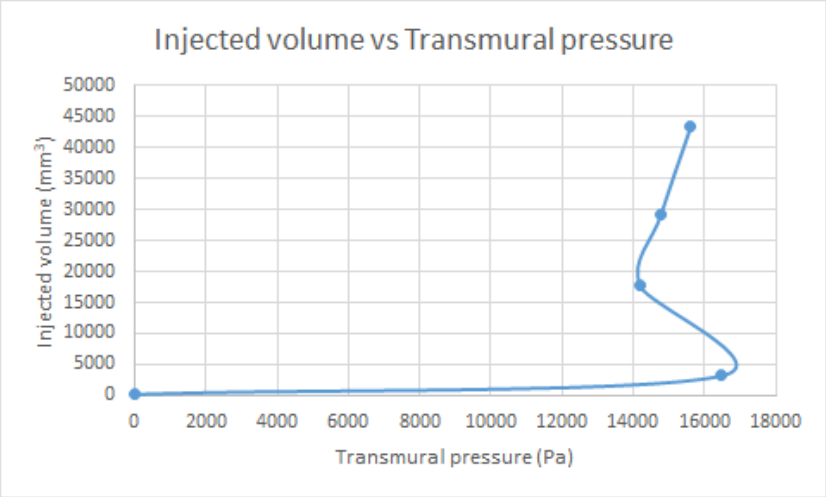

Figure 5.50: Injected volume vs Transmural pressure (Test 7).

The behaviour of the balloon was in all similar to that of previous tests, that is, the transmural pressure increases from 0.00 Pa (when there is no pressure applied to the object under study) until the time when the resistance of the balloon is exceeded. From there, the transmural pressure drops a little bit but soon starts to increase again, however in small steps. The injected volume assumes the opposite behaviour, starting to increase in small steps of volume and from the moment that the peak of pressure is reached, the injected volume increases considerably.

Comparing the transmural pressure and injected volume values from both tests (Test 5 | Test 7) through Tables 5.5 and 5.7, it may be noticed that they are all very similar. This happens because the pressurizing rate only influence the duration of the test, that is, a higher pressurizing rate requires less time for the test to be completed.

The measurements performed in this test were very accurate and consistent with mean standard deviation about 3% for both pressure and volume values.

After the tests with water, and comparing the results with ones for the tests using air, it can be affirmed that the pressure values are very similar and the injected volume values are slightly higher.

It can be concluded that the performance of the device regarding the ability to perform different displacements taking into consideration the same pressurizing rates or to perform the same displacement taking into consideration different pressurizing rates is the same, whether water or air is used as fluid.

5.1.3 Long balloon inflated with saline solution

In order to evaluate the influence of the density of the fluid in the performance of the device, a test was repeated using saline solution (Test 8) since this fluid as a density of 1.09 g/cm^3 and water as a density of 1.00 g/cm^3 - at 25^{o}C - [31]. In that way, the device was required to move the plunger of the syringe 30 mm, in the direction of pressurizing, with a pressurizing rate of 18850 mm^3/s, full

step mode and to perform 4 readings of the transmural pressure value inside the balloon, during the task. The collected photographs and their 3D reconstructions are in the Figures 5.51-5.55 and the values of the transmural pressure and the injected volume are expressed in Table 5.8 and in Figures 5.56 and 5.57.

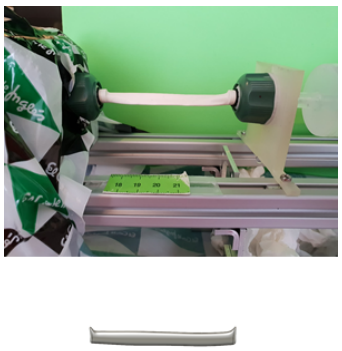

Figure 5.51: Balloon deformation state at the initial time (Test 8).

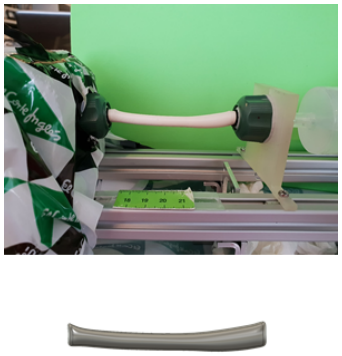

Figure 5.52: Balloon deformation state at the second transmural pressure measurement (Test 8).

Figure 5.53: Balloon deformation state at the third transmural pressure measurement (Test 8).

Figure 5.54: Balloon deformation state at the fourth transmural pressure measurement (Test 8).

Figure 5.55: Balloon deformation state at the fifth transmural pressure measurement (Test 8).

Table 5.8: Transmural pressure and injected volume values (Test 8)

Reading number	Transmural pressure (Pa)	Injected volume (mm^3)
1	0.00±0.00	904.852±23.255
2	18240.00±370.27	2512.696±83.673
3	16550.00±554.43	8778.793±409.970
4	11310.00±197.93	15640.000±400.384
5	11030.01±446.72	19970.000±449.325

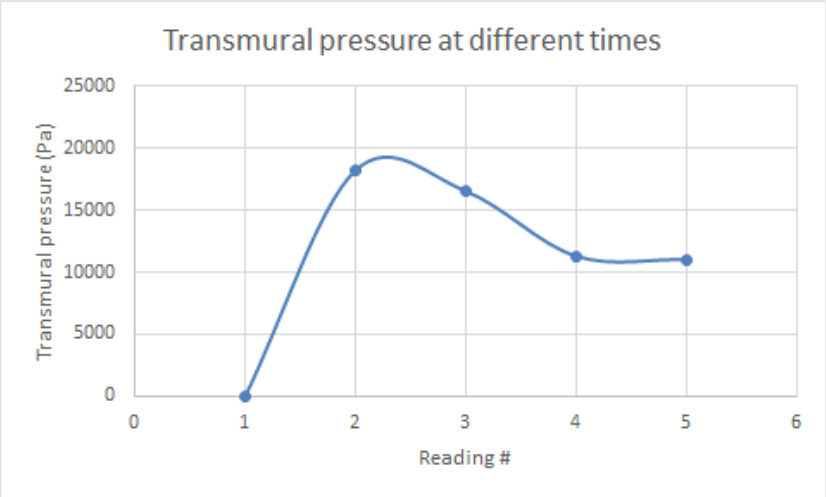

Figure 5.56: Transmural pressure at different times (Test 8).

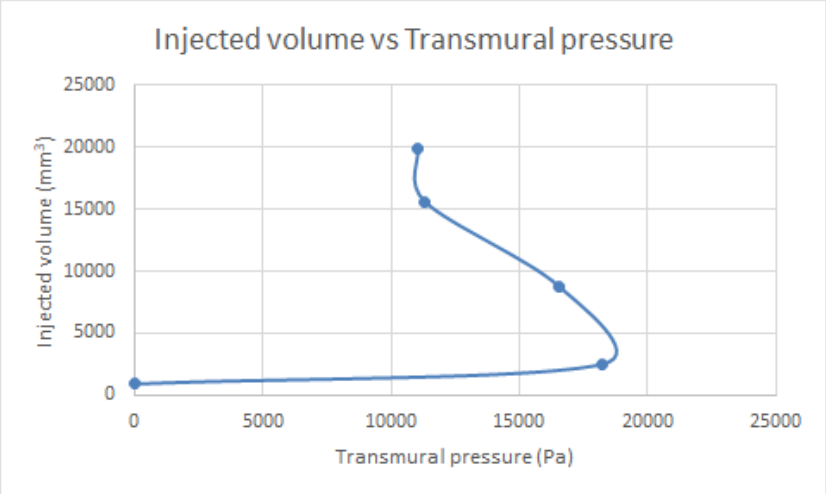

Figure 5.57: Injected volume vs Transmural pressure (Test 8).

Once again, comparing the tests carried out with air and water, the behaviour of the transmural pressure and injected volume is the same, exhibiting the same characteristics before and after the moment when the balloon resistance force is exceeded.

Looking for Tables 5.6 and 5.8, which contain the values of the transmural pressure and the values of the injected volume for the same test using water and saline solution, respectively, it can be assumed that using saline solution instead of water to pressurize the balloon has no influence on the final volume since the values collected for both tests (both pressure values and injected volume values) are very similar.

The mean standard deviation was about 3% for both measures and, so, it can be affirmed that the measurements are very accurate between each assay.

5.2 Tests with organic structures

In order to evaluate the performance of the Injection Pump device in the pressurization of organic structures, a test in a porcine aorta was executed.

Due to the lack of time and the difficult access to an intact blood vessel of an animal, like pig, chicken or rabbit, this was the unique test performed in organic tissue.

The apparatus was instructed to displace the plunger of the syringe by 60 mm, at 18850 mm^3/s, full step mode and to perform 4 readings of the transmural pressure. The pressurizing fluid used was saline solution, since it has a density value more similar to that of blood (1.09 g/cm^3 and 1.06 g/cm^3, respectively) [32].

The collected images and their 3D reconstructions are in Figures 5.58-5.62 and the values of the transmural pressure and injected volume are in Table 5.9 and in Figures 5.63 and 5.64.

As it was not possible to perform more than one assay for this test, the transmural pressure and injected volume values are not presented in the mean $\pm$ standard deviation form, being only the collected values presented.

Figure 5.58: Porcine aorta deformation state at the initial time.

Figure 5.59: Porcine aorta deformation state at the second transmural pressure measurement.

Figure 5.60: Porcine aorta deformation state at the third transmural pressure measurement.

Figure 5.61: Porcine aorta deformation state at the fourth transmural pressure measurement.

Figure 5.62: Porcine aorta deformation state at the fifth transmural pressure measurement.

Table 5.9: Transmural pressure and injected volume values (Porcine Aorta test)

Reading number	Transmural pressure (Pa)	Injected volume (mm^3)
1	0.00	11880.000
2	6790.00	12290.000
3	13360.00	16610.000
4	13580.00	18410.000
5	13770.00	19230.000

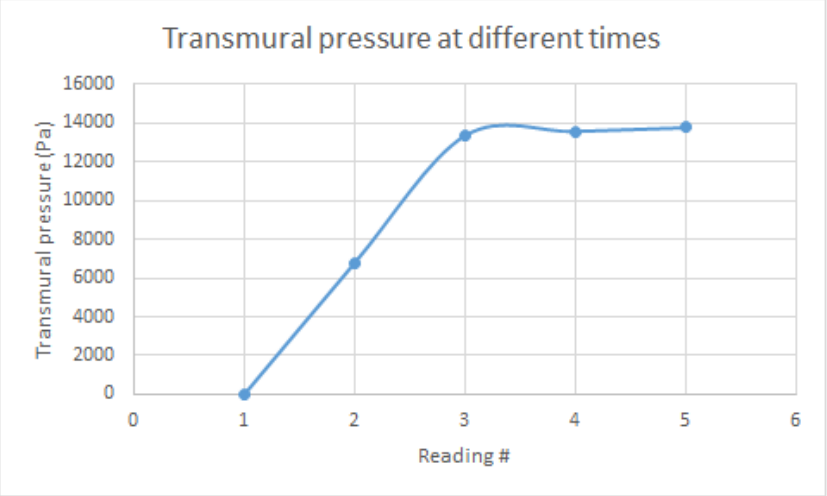

Figure 5.63: Transmural pressure at different times (Porcine aorta test).

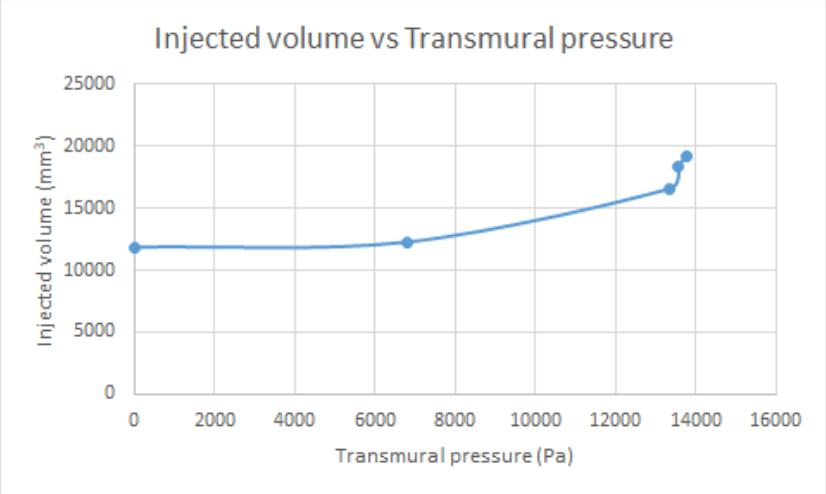

Figure 5.64: Injected volume vs Transmural pressure (Porcine aorta test).

The reference length at zero transmural pressure was 90 mm.

Looking at Figure 5.64 and to Figures 5.58-5.62, it is notable that the volume of fluid within the artery has increased over time. The transmural pressure had an initial value of 0.00 Pa, that is, no pressure was being applied to the vessel and the volume (of air) inside of it was of 11880.000 mm^3.

Over time, the volume of saline solution inside the aorta increased and, with it, the transmural pressure on the walls of the vessel. The injected volume of fluid at the end of the test was of 19230.000 mm^3 and the transmural pressure took the value of 13770.00 Pa ($\sim$103 mm Hg).

These results are in agreement with what is expected, since both the transmural pressure and the volume of fluid within the artery increased with time. Unlike the results obtained with the long

balloon, with any of the pressurizing fluids used, there was no pressure drop because the walls of the two structures have different behaviour under pressure.

Chapter 6

Conclusions and future work

6.1 Conclusions

The construction of the Injection Pump device arises with the need to investigate how the BMS can be redesigned and improved, so that they are again widely used. This led to the need of performing mechanical tests on arteries, to analyze their behaviour under pressure and, in the future, to analyze how the set composed by the artery and the stent behaves when subjected to physiological pressures.

The tests performed to the balloons and to the porcine aorta proved that the developed apparatus is completely able to inflate tubular and organic structures and that the behaviour of the balloons under pressure is completely different of the behaviour of the animal tissue. Whereas for the porcine aorta there is a continuous increase in the transmural pressure and in the volume of fluid injected over time, into the balloon these two variables assume different behaviors before and after the transmural pressure exceeds the value of resistance of the balloon to deformation. Before the mentioned event, the transmural pressure increases at considerable intervals up to a certain value (value of the balloon's resistance force to the deformation) and then is followed by a depression. After this depression, the transmural pressure increases again but at smaller intervals. In relation to the injected volume of fluid, it has an opposite behavior to that of the transmural pressure, increasing initially at small intervals and after the transmural pressure exceeds the resistance of the balloon, increases in considerable amounts intervals, since less force is required to introduce the same volume of fluid in the balloon.

One of the aspects to be improved is to increase the maximum volume that the apparatus can inject into the tubular structure so that could be possible to test the maximum volume and rupture pressure of the arteries, for example. Another drawback of the apparatus is that, when a test is repeated at a higher pressurizing rate, it encounters a greater resistance to movement and slides. One way to solve this problem would be to use a stepper motor with a higher torque.

The objectives proposed for this dissertation, that can be consulted in chapter 1 (section 1.4), were reached except one. An automated testing system for pressured biological systems was assembled and it is fully functional; the efficacy of the testing system was validated by performing

inflation tests to long balloons and to a piece of porcine aorta; an experimental protocol, for biological materials, adapted to the system was created. The unique goal that was not reached was the study of the mechanical characterization of biological vessels (arteries or veins) as test/application proof of the system. However, the missing part is easily reached and can be performed in a short future.

The concept of the device is not completely new but having the three different components (an inflation system, fully automated and programmable; a pressure measurement system, consisting of a direct measurement since the sensor is inside the vessel; a deformation measurement system, with 3D reconstruction of vessel deformation) on a single solution is innovative and there is a huge potential to extend the same testing system to different biological systems, as the urinary system and study of the mechanical properties of the urethra.

6.2 Future work

The future work that could be done with the Injection Pump device to emphasize its importance and meet the main motivation of its construction, is:

(i) perform a full test to organic structures and validate the results

(ii) perform tests in other types of animal tissue, such as cow, sheep or dog

(iii) extend the same testing system to different biological systems as the urinary system (study of the mechanical properties of the urethra) or the circulatory system (study of the mechanical properties of arteries and veins)

Since there was no opportunity to perform the mechanical characterization of biological vessels (arteries or veins) as test/application proof of the system, the protocol should be the following:
1. Obtain pieces of porcine thoracic aorta and keep it at 5^{o}C, in saline solution, if it was not used to perform the test immediately after harvest
2. Remove the peripheral, loose connective tissues from the adventitia and keep the aortic branches intact
3. Ligate all the aortic branches with nylon or suture thread (to prevent the leakage of pressurizing fluid)
4. Measure the reference length at zero transmural pressure
5. Apply a pre-conditioning to the specimens performing 10 cycles of inflation pressure over the range 5–25 kPa and at a frequency of 0.5 Hz
6. Pressurize and depressurize the specimen five times over a transmural pressure range from 10-160 mm Hg ($\sim$1.33-21.33 kPa), at room temperature (frequency of 1/110 Hz)
7. With the collected pictures, perform the 3D reconstruction with Fusion 360 software
8. Drawn the Transmural pressure over time and Injected volume vs Transmural pressure graphs
9. Validate the results with the works of [21] and [9]

Appendix A

Protocol for using the Injection Pump device

A.1 Summary

The Injection Pump device is an inflation system testing device with application to organic structures under pressure and it is presented in Figure A.1. The system is composed by three different components: an inflation system, a pressure measurement system and a deformation system.

A stepper motor is the base component of the system and, in this way, the control of the whole system is controlled by the motor. When the motor moves, it pushes the plunger of a syringe, pumping forward/backward, inducing the increase or the decrease of the transmural pressure inside the tissue under study, respectively.

The transmural pressure inside the vessel (or its substitute) is continuously measured by a pressure sensor and the 3D reconstruction of the tubular object under study is made from the pictures captured at the time of each pressure reading. These photos are used in the software ***Fusion 360***, from Autodesk, to perform the 3D reconstruction of the tubular vessel and to measure the volume of fluid inside it.

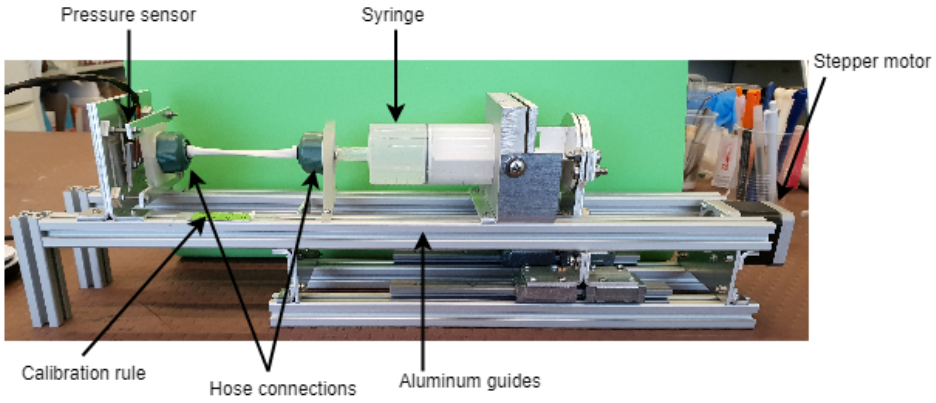

Figure A.1: Injection Pump device

A.2 Softwares

A.2.1 Required softwares

In order to use the Injection Pump device, it is necessary to have installed on your computer three softwares: MATLAB, ARDUINO IDE and FUSION 360.

The first one can be bought or downloaded with a student or professional license (https://www.mathworks.com/downloads/). The Arduino IDE can be downloaded for free from https://www.arduino.cc/en/Main/Software. Finally, Fusion 360 can be downloaded with a student license too, from https://www.autodesk.com/products/fusion-360/students-teachers-educators. The installing instructions available on the page must be followed.

A.2.2 Installing libraries

A.2.2.1 Matlab and required libraries

To use the Matlab for the operation of this device, it is needed to install the Arduino Support Package. If you don't have this package installed yet, you should follow the steps described below.

1. Go to **HOME** and then **Add-ons**, where you should select **"Get Hardware Support Packages"**
2. **"Install from Internet"** and the **"Next"**
3. Choose **"Arduino"** from the list that is available and check **"Install"** in the available package **"Acquire inputs and send outputs on Arduino Uno, Due and more"** and click **"Next"**

4. Do LOGIN on your Matlab account
5. Check **“I accept”** and then **“Next”**
6. Click **“Next”** and then **“Install”**
7. Allow the Matlab to make changes in your PC
8. Click on **“Continue”**
9. Then **“Next”**
10. **“Next”** again and **"Finish"**

A.2.2.2 Arduino and required libraries

To run the Arduino code, it is necessary to include specific libraries. In this case, the library to allow the operation of the motor and another to the operation of the pressure sensor.

The user installed libraries are stored in the “libraries” folder, inside the Arduino sketch folder. On Windows systems should be located in “My Documents/Arduino”, on Mac computers in "∼/Documents/Arduino” and on Linux in “∼/Arduino/sketchbook”. Look for the Arduino folder on your pc and open it.
The AccelStepper library, necessary to the motor operation, can be downloaded from https://www.arduinolibraries.info/libraries/accel-stepper. After the download, you just need to unzip it and drag the folder to your “libraries” folder of your Arduino sketch folder.

The next step is the download of the MS5803 software archive from https://github.com/sparkfun/MS5803-14BA_Breakout/archive/master.zip. After complete the download, you should open it and open the folder “MS5803-14BA_Breakout-master”, then “Libraries” and then “Arduino”. After these, you should see a folder called “SFE_MS5803_14BA_I2C”, which you should drag from the .zip folder to your “libraries” folder of your Arduino sketch folder.

These libraries are already included in the beginning of the Arduino code, through these instructions:

```
#include <AccelStepper.h>
#include <SparkFun_MS5803_I2C.h>
```

A.2.3 How to use the softwares

A.2.3.1 Arduino

After opening the Arduino code, you need to:

1. Connect the Arduino to the computer through its USB cable
2. Go to the Control Panel and then Device Manager

3. Check the Port (COM and LPT) section

4. Check the serial port number being used – e.g. “Arduino Uno (COM3)”

Then, in the Arduino IDE, you should go to TOOLS and check if the Board, the Processor and the Door are correctly attributed.

After that, you just need to send the code to the board. For that, you just need to click on the SEND button.

A.2.3.2 Matlab

After opening the Matlab code, you just need to run the code by clicking on the RUN button, available in the EDITOR menu. The interface to control the device is going to appear automatically.

A.2.3.3 Fusion 360

The software Fusion 360 is used to perform the 3D reconstruction of the tubular structures under study and to estimate the volume of fluid inside it.

In order to plot the injected volume versus pressure, you need to reconstruct structure with the photos taken during the test. To do that, you only need to perform the following steps in Fusion 360 work area.

1. INSERT and then Attached Canvas

2. Select the plane of the axis that you want to work on, upload the photo that you want to reconstruct, adjust the photo according the main axis and click on “OK”

3. Go to BROWSER, then Canvases” and “Calibrate” to calibrate the dimensions of your object

4. To build the form, go to CREATE and then select the geometric solid that is going to be the starting point of your sketch

5. After that, go to MODIFY and adjust the corners and edges of your solid according with your structure

6. To finish the model, click on FINISH FORM

7. To obtain the volume of the model, go to BROWSER, then BODIES and finally, PROPERTIES, where you can consult the desired property

To obtain the final graph, you just need to follow the previous steps for all photos.

A.3 Rules to use the interface

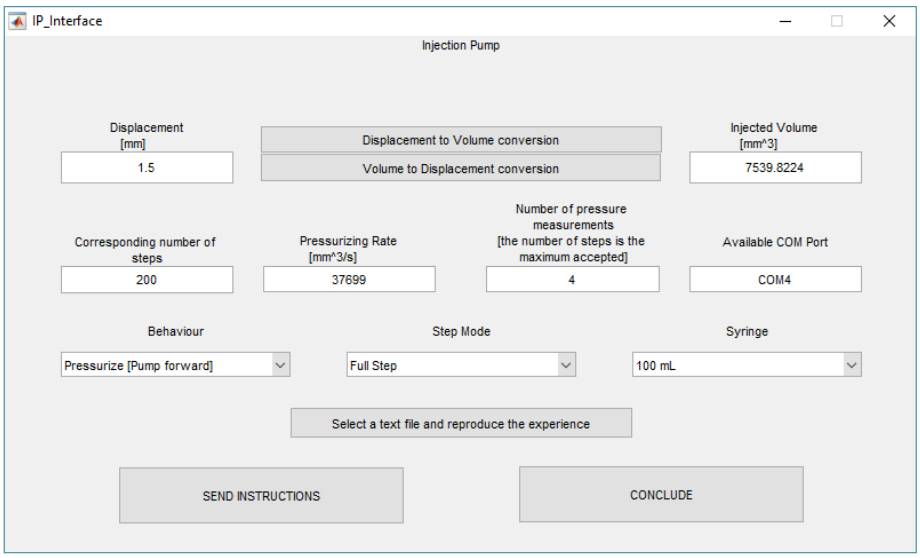

Figure A.2: Matlab-Arduino interface

To perfectly control the device, some rules must be followed when using the interface presented in figure A.2. Some information is given below.

Displacement: this parameter represents the displacement of the plunger of the syringe and must be written in millimeters, in the first box.

Injected volume: in this place you should write the volume of fluid that you want to be injected by the syringe into the vessel and this parameter has cubic millimeters as unities.

If you only know what the displacement that you want is, you can convert it into the correspondent injected volume, pressing the "Displacement to Volume conversion". Otherwise, if you only know the volume that you want to be injected and don't know how to translate it into displacement, you just need to press the "Volume to Displacement conversion" button.

Syringe information:
- For the 10 mL syringe, one full revolution of the motor, moves the syringe 1.5 millimeters and injects a volume of 471.2389 cubic millimeters.
- For the 20 mL syringe, one full revolution of the motor, moves the syringe 1.5 millimeters and injects a volume of 1885 cubic millimeters.
- For the 100 mL syringe, one full revolution of the motor, moves the syringe 1.5 millimeters and injects a volume of 7539.8 cubic millimeters.

Corresponding number of steps: the value registered in this box is merely informative for you to know the number of steps the motor moves depending on the displacement that you asked. It is also useful to understand what is the maximum number of pressure readings you can perform since this maximum is equal to the number of steps that the motor will move.

Pressurizing rate: represents how many cubic millimeters of fluid are injected, per second, in the vessel and has mm^3/s as unities. - For the 10 mL syringe, the maximum pressurizing rate is 2356.2 mm^3/s. - For the 20 mL syringe, the maximum pressurizing rate is 9424.8 mm^3/s. - For the 100 mL syringe, the maximum pressurizing rate is 37699 mm^3/s.

Number of readings: insert how many times you want the transmural pressure to be read during the displacement of the motor.

Available COM Port: you need to write in the box in the format "COMx", being x the number of the serial port, as it is in the example above – "COM3". This information is collected when the Arduino code is sent to the board, being the procedure described in section 2.3.1.

Behaviour: you may choose if you want to pressurize (pump forward) or depressurize (pump backward) your study object. This choice must be done in the available pop-up menu called "Behaviour".

Step Mode: the step mode can be chosen in the Step Mode menu. The options are: Full, Half, Quarter, Eighth and Sixteenth step and you must choose one of the available options.

Syringe: you may choose, in the menu, which is the volume of the syringe that you are using. After fulfilling all the requirements, press the START button, to send the instructions to the Arduino.

With this device you can order it to perform more than one task. For this, you just need to complete all the parameters mentioned above and press START after the instruction is completed. At send the task or the set of tasks desired, click the CONCLUDE button.

Select a text file and reproduce the experience

It is possible to reproduce an experience made before by this device. For this, you just need to press the "Select a text file and reproduce the experience" button and select the text file generated by MATLAB at the end of that experience. MATLAB will read the instructions sent to Arduino and reproduce them.

A.4 Outputs of each experience

At the end of each experience, a text file is created, with the instructions that you ask the device to perform and with the transmural pressure values registered over time - Figure A.3. It is this file that you need to select if you want to reproduce the same tasks, later. This feature allows the tasks to be reproducible. Beyond the text file, a set of pictures is collected. These photos will be need to perform the 3D reconstruction of the object under study and its volume, in the Fusion 360 software - Figure A.4.

The most relevant information to be drawn from the experiments is how the transmural pressure varies over time and how the injected volume varies with the transmural pressure. In this way, these data are presented in the form of a graph.

Figure A.3: Text file generated at the end of a task

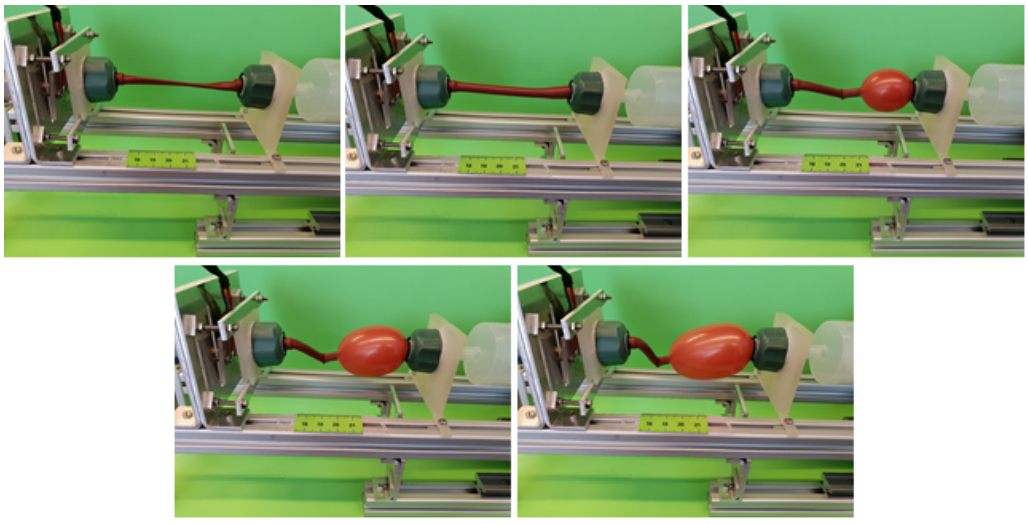

Figure A.4: Example of a set of images collected at the end of a task

References

[1] NIH. SEER Training:Classification & Structure of Blood Vessels. URL: https://training.seer.cancer.gov/anatomy/cardiovascular/blood/classification.html.

[2] M. Sato, H. Niimi, A. Okumura, H. Handa, K. Hayashi, and K. Moritake. Axial mechanical properties of arterial walls and their anisotropy. *Medical & Biological Engineering & Computing*, 17(2):170–176, 1979. doi:10.1007/BF02440925.

[3] Kozaburo Hayashi, Keiichi Takamizawa, Takao Nakamura, Tadashi Kato, and Nobuko Tsushima. Effects of elastase on the stiffness and elastic properties of arterial walls in cholesterol-fed rabbits. *Atherosclerosis*, 66(3):259–267, 1987. doi:10.1016/0021-9150(87)90069-4.

[4] K. Hayashi, M. Sato, H. Handa, and K. Moritake. Biomechanical study of the constitutive laws of vascular walls. *Experimental Mechanics*, 14(11):440–444, 1974. URL: http://link.springer.com/10.1007/BF02324024, doi:10.1007/BF02324024.

[5] Walter C P M Blondel, Jacques Didelon, Gérard Maurice, Jean-pierre P Carteaux, Xiong Wang, and J F Stoltz. Investigation of 3-D mechanical properties of blood vessels using a new in vitro tests system: results on sheep common carotid arteries. *IEEE transactions on bio-medical engineering*, 48(4):442–51, 2001. URL: http://www.ncbi.nlm.nih.gov/pubmed/11322532, doi:10.1109/10.915710.

[6] Thomas E Carew, Ramesh N Vaishnav, J Dali, Greenville Avenue, Permissions Permissions, Rights Desk, Lippincott Williams, and Phone Fax. Compressibility of the Arterial Wall The online version of this article , along with updated information and services , is located on the World Wide Web at : Compressibility of the Arterial Wall. 1968.

[7] Christian A. J. Schulze-Bauer, Christian Morth, and Gerhard A. Holzapfel. Passive Biaxial Mechanical Response of Aged Human Iliac Arteries. *Journal of Biomechanical Engineering*, 125(3):395, 2003. URL: http://biomechanical.asmedigitalcollection.asme.org/article.aspx?articleid=1410289, doi:10.1115/1.1574331.

[8] Philip B. Dobrin. Biaxial anisotropy of dog carotid artery: Estimation of circumferential elastic modulus. *Journal of Biomechanics*, 19(5):351–358, 1986. doi:10.1016/0021-9290(86)90011-4.

[9] Jungsil Kim and Seungik Baek. Circumferential variations of mechanical behavior of the porcine thoracic aorta during the inflation test. *Journal of Biomechanics*, 44(10):1941–1947, 2011. URL: http://dx.doi.org/10.1016/j.jbiomech.2011.04.022, doi:10.1016/j.jbiomech.2011.04.022.

[10] WHO. WHO | Cardiovascular diseases (CVDs), 2017. URL: http://www.who.int/mediacentre/factsheets/fs317/en/.

[11] NIH. What Is Atherosclerosis? - NHLBI, NIH. URL: https://www.nhlbi.nih.gov/health/health-topics/topics/atherosclerosis.

[12] NIH. How Is Atherosclerosis Treated? - NHLBI, NIH. URL: https://www.nhlbi.nih.gov/health/health-topics/topics/atherosclerosis/treatment.

[13] Gerhard A Holzapfel, Gerhard Sommer, Christian T Gasser, Peter Regitnig, A Gerhard, Gerhard Sommer, Christian T Gasser, and Peter Regitnig. Determination of layer-specific mechanical properties of human coronary arteries with nonatherosclerotic intimal thickening and related constitutive modeling. pages 2048–2058, 2005. doi:10.1152/ajpheart.00934.2004.

[14] Kozaburo Hayashi. Experimental approaches on measuring the mechanical properties and constitutive laws of arterial walls. *Journal of biomechanical . . .* , 115(November 1993):481–488, 1993. URL: http://biomechanical.asmedigitalcollection.asme.org/article.aspx?articleid=1399600, doi:10.1115/1.2895528.

[15] MEE. Tension and Compression Testing | Tension and Compression Failure Analysis | Tension and Compression Material Analysis | ToF-SIMS. URL: https://www.mee-inc.com/hamm/tension-and-compression-testing/.

[16] C. J. Chuong and Y. C. Fung. Compressibility and constitutive equation of arterial wall in radial compression experiments. *Journal of Biomechanics*, 17(1):35–40, 1984. arXiv:79952362731, doi:10.1016/0021-9290(84)90077-0.

[17] C. Lally, A. J. Reid, and Patrick J. Prendergast. Elastic behavior of porcine coronary artery tissue under uniaxial and equibiaxial tension. *Annals of Biomedical Engineering*, 32(10):1355–1364, 2004. doi:10.1114/B:ABME.0000042224.23927.ce.

[18] Alireza Karimi, Mahdi Navidbakhsh, Ahmad Shojaei, and Shahab Faghihi. Measurement of the uniaxial mechanical properties of healthy and atherosclerotic human coronary arteries. *Materials Science and Engineering C*, 33(5):2550–2554, 2013. URL: http://dx.doi.org/10.1016/j.msec.2013.02.016, doi:10.1016/j.msec.2013.02.016.

[19] M. Pagani, I. Mirsky, H. Baig, W. T. Manders, P. Kerkhof, and S. F. Vatner. Effects of age on aortic pressure-diameter and elastic stiffness-stress relationships in unanesthetized sheep. *Circulation Research*, 44(3):420–429, 1979. doi:10.1161/01.RES.44.3.420.

[20] B S Gow and C D Hadfield. The elasticity of canine and human coronary arteries with reference to postmortem changes. 45:588–594, 1979.

[21] Steven P. Marra, Francis E. Kennedy, Jeffrey N. Kinkaid, and Mark F. Fillinger. Elastic and rupture properties of porcine aortic tissue measured using inflation testing. *Cardiovascular Engineering*, 6(4):123–131, 2006. doi:10.1007/s10558-006-9021-5.

[22] Véronique Laterreur, Jean Ruel, François A. Auger, Karine Vallières, Catherine Tremblay, Dan Lacroix, Maxime Tondreau, Jean Michel Bourget, and Lucie Germain. Comparison of the direct burst pressure and the ring tensile test methods for mechanical characterization of tissue-engineered vascular substitutes. *Journal of the Mechanical Behavior of Biomedical Materials*, 34:253–263, 2014. doi:10.1016/j.jmbbm.2014.02.017.

[23] Christian A. J. Schulze-Bauer, Peter Regitnig, and Gerhard A. Holzapfel. Mechanics of the human femoral adventitia including the high-pressure response. *American Journal of Physiology - Heart and Circulatory Physiology*, 282(6):H2427–H2440, 2002. URL: http://ajpheart.physiology.org/lookup/doi/10.1152/ajpheart.00397.2001, doi:10.1152/ajpheart.00397.2001.

[24] AHA. What Is a Stent? *American Heart Association*, 2017. URL: https://www.heart.org/idc/groups/heart-public/@wcm/@hcm/documents/downloadable/ucm{_}300452.pdf.

[25] Hidehiko Hara, Masato Nakamura, Julio C. Palmaz, and Robert S. Schwartz. Role of stent design and coatings on restenosis and thrombosis. *Advanced Drug Delivery Reviews*, 58(3):377–386, 2006. doi:10.1016/j.addr.2006.01.022.

[26] OrbusNeich. Types of Coronary Stents | OrbusNeich. URL: https://www.orbusneich.com/en/patient/types-coronary-stents-0.

[27] Sandy N Shah. Coronary Bare-Metal Stent: Products, Design Features, Indications. URL: https://emedicine.medscape.com/article/2009987-overview.

[28] S. G. Sakka, A. Harzheim, and F. Wappler. Sudden hypoxaemia in a critically ill adult patient: Anomalous drainage of the upper left pulmonary vein. *British Journal of Anaesthesia*, 102(3):434–435, 2009. doi:10.1093/bja/aen397.

[29] Dean J. Kereiakes, Yoshinobu Onuma, Patrick W. Serruys, and Gregg W. Stone. Bioresorbable Vascular Scaffolds for Coronary Revascularization. *Circulation*, 134(2):168–182, 2016. doi:10.1161/CIRCULATIONAHA.116.021539.

[30] Kleanthis Theodoropoulos and Roxana Mehran. Dual-Therapy Stenting: The Next Step in the Evolution of Stent Design. URL: https://www.healio.com/cardiology/intervention/news/print/cardiology-today-intervention/{%}7Bd6561e10-c5c0-4c9d-afbd-f65922406b27{%}7D/dual-therapy-stenting-the-next-step-in-the-evolution-of-stent-design.

[31] W. L. Switzer. Density of Water. URL: https://chemistry.sciences.ncsu.edu/resource/H2Odensity{_}vp.html.

[32] Michael Shmukler. Density of Water. URL: https://chemistry.sciences.ncsu.edu/resource/H2Odensity{_}vp.html.